Polarizability as a Single Parameter to Predict Octanol-water Partitioning Coefficient and Bioconcentration Factor for Persistent Organic Pollutants

By Xiaolei Li

A thesis submitted to the
School of Graduate Studies
in partial fulfillment of the
requirement for the degree of
Master in Science

Department of Chemistry
Memorial University of Newfoundland

July 2016

St. John's Newfoundland

Abstract

Surface microlayer (SML) is critical to various Earth system processes due to its unique physiochemical properties. One of main concerns regarding SML is regarding the persistent organic pollutants (POPs) partition. This process is vital in understanding air-sea exchange and, to a large extent, the global transportation of POPs. POPs have potential significant impacts on human health and on the aquatic environment, and their properties are critical to understanding and predicting the environmental fate of persistent chemicals. To study the partition properties of SML, it would be interesting to study two related properties of POPs, the octanol-water partitioning coefficient and the bioconcentration factor, both of which serve as criteria to determine the accumulation of a compound. Although numerous models have been previously published to predict K_{OW} and/or BCF, the results are not statistically robust. The resulting linear free energy relationships obtained from poly-parameters on a strictly statistical basis, although they yield good results, may cause chance correlation and bear no physico-chemical meaning. Given that dispersion forces are the dominant inter-molecular interaction in non-polar compounds and that molecular polarizability can describe dispersion forces in condensed phase partitioning, we developed a method to predict K_{OW} and BCF using molecular polarizability as a single parameter. The polarizabilities of non-polar compounds with available consistent measurement data were calculated using density functional theory with B3LYP functionals and the 6-311g(d, p) basis set in Gaussian program (09 version or 03 version); a single-parameter structure-activity relationship was then separately derived from the modeled compounds using a linear least-squares regression for K_{OW} and BCF. We modelled BCF in the real world for a microorganism and a fish (*Cyprinos Carpio*). A comparison with data from other models showed that this is a simple but effective method to predict K_{OW} and BCF for non-polar compounds. The

prediction power for BCF using this method in microorganism shows that polarizability would be a good indication for partition SML due to the fact that both microorganism and SML can be seen as biofilms. Sampling POPs in the SML is a challenge to the scientist; a glass plate with a vacuum squeegee was developed to efficiently collect a freshwater SML sample from a local pond for GC-MS analysis of POPs.
Key words: Polarizability; octanol-water partition coefficient; bioconcentration factor; surface microlayer; persistent organic pollutant

Acknowledgements

Firstly, I would like to express my sincere gratitude to my advisors Dr. Cora Young and Dr. Robert Helleur for the continuous support of my masters' study and related research, and for their patience, motivation, and immense knowledge. Their guidance helped me in all the time of research and writing of this thesis. Also, their support of my life is a treasure which will give me the courage to face all life's challenges.

Besides my co-supervisors, I would like to thank the rest of my supervisory committee that being Dr. Chris Rowley for his comments and encouragement, but also for the hard questions which incented me to widen my research from various perspectives.

Also, my sincere gratitude goes to Dr. Jamie Donaldson, professor in University of Toronto, for his contributions to Chapter 2 and 3. I am extremely grateful for his assistance and suggestions in the research.

And I am very thankful to Dr. Cora Young's group, without their support, it would not be possible to conduct this research.

I also would like to thank my husband Dr. Yang Zhang for his support both in life and research, to my son Alexander Lee, who gave me the power to finish a master thesis instead of a PhD thesis, and to my families for their unconditional support.

Table of Contents

Abstract i

Acknowledgements iii

Table of Contents iv

List of Tables vii

List of Figures viii

List of Abbreviations and Symbols x

Chapter 1. Introduction 1

1.1. Surface Microlayer 1

1.2. Persistent organic pollutants 2

1.2.1. Definition 2

1.2.1.1. Persistent in environment 3

1.2.1.2. Bioaccumulation 3

1.2.1.3. Long-range environmental transportation 4

1.2.1.4. Toxicity 5

1.2.2. POPs present in SML 6

1.3. Octanol–water partition coefficient 6

1.3.1. Experimental methods used to determine K_{OW} 7

1.3.1.1. Flask shaking method 7

1.3.1.2. Generator Column Method 7

1.3.1.3. Slow stirring method 8
1.3.1.4. Chromatography 8
1.3.2. Computational methods 9
1.3.2.1. Substructure approaches 10
1.3.2.2. Whole molecule approach 12
1.4. Bioconcentration factor 13
1.4.1. Experimental methods 14
1.4.2. Computational Methods 15
1.5. SML sampling method 16
1.5.1. Plate sampler 16
1.5.2. Mesh screen and membrane surface methods 18
1.5.3. Rotating drum method 18
1.5.4. Rotating glass disk method 19
1.6. Objectives 21
Chapter 2. Molecular polarizability as a single parameter to predict Octanol-water Partition Coefficient 22
2.1. Introduction 22
2.2. Methods 23
2.3. Thermodynamic Premise 25
2.4. Results and Discussion 26

Chapter 3. Molecular polarizability as a single parameter to predict Bioconcentration Factor 32

3.1. Introduction 32

3.2. Methods 33

3.2.1. For microorganism BCF 33

3.2.2. For fish BCF 33

3.3. Results and Discussions 34

Chapter 4. An improved glass plate surface microlayer sampling method using an auto squeegee..... 39

4.1. Introduction 39

4.2. Materials and Method 40

4.1.1 Materials 40

4.1.2 Sample Collection and Preparation 41

4.1.3 Solid Phase Extraction (SPE) Methodology 41

4.1.4 Gas Chromatography-Mass Spectrometry detection 42

4.3. Results and Discussions 42

Chapter 5. Conclusions and Future Work 46

References 48

Appendices 57

List of Tables

Table 4.1 Ion monitoring in PBDEs experiments and results 45

Table S.1 Molecular polarizability calculated with B3LYP functionals and the 6-311g(d,p) basis set 57

Table S.2 Compounds used to correlate molecular polarizability and *log* K_{OW}, predicted results are indicated. 61

Table S.3 Compounds used to correlating molecular polarizability and *log* BCF, predicted results are indicated. 68

Table S.4 Compouds used to correlate molecular polarizability and *log* BCF in microorganism 70

List of Figures

Figure 1.1 Schematic model of the structure of the air-water interface (Cunliffe, 2011)..... 1

Figure 1.2 POPs Global migration Process (Wania & Mackay, 1996) 5

Figure 1.3 The predicted and experimental *log* BCF values obtained with the CAESAR model (Registration, 2006) 17

Figure 1.4 Glass plate sampler. (a) shows the glass plate sampler (reproduced from Van Pinxteren et al., 2012) while (b) illustrates removal of microlayer, reproduced from Harvey & Burzell (2003). 18

Figure 1.5 Rotating drum method for sampling SMLreproduced from Harvey (2003) 19

Figure 1.6 (a) Photograph of a rotating disk microlayer sampler. (b) Schematic diagram showing glass disks with Teflon wipers in between. (c) Photograph of the glass disk module. (d) Photograph taken from the bottom of the vessel, indicating the location of the glass-disk module, adapted without permission from Shinki et al. 2012. 20

Figure 2.1 Correlation between median measured *log* K_{OW} (from Reference 1 and references therein) and calculated molecular polarizability. Red squares indicate eleven tetrachlorobiphenyl isomers; a linear regression through all data is shown by the black line. 27

Figure 2.2 Predicted *log* K_{OW} from calculated polarizability compared to measured *log* K_{OW} for 86 compounds. The training set (n=64) is shown in grey, the 1:1 line (black) and 1:1 line ± 1 *log* unit (grey) are shown as well. The validation set (n=22) is shown as red and blue symbols, where the red symbols display the mean ± standard error when there are several measurements, and the blue shows the cases of a single measurement ± its assumed error range. 28

Figure 2.3 Predicted *log* K_{OW} from calculated polarizability (red diamonds), and commonly cited (open triangles and squares) or recent (open circles) poly-parameter predictive methods compared to measured *log* K_{OW} for polychlorinated biphenyls. The 1:1 line (black); 1:1 line ± 0.5 *log* unit (dark grey) and 1:1 line ± 1 *log* unit (light grey) are illustrated..... 29

Figure 2.4 Predicted *log* K_{OW} from calculated polarizability and commonly cited predictive methods for fluorinated compounds. The 1:1 line (black); 1:1 line ± 0.5 *log* unit (dark grey) and 1:1 line ± 1 *log* unit (light grey) are illustrated..... 30

Figure 3.1 Correlation between molecular polarizability and measured *log* BCF in microorganism(species unspecified)..... 34

Figure 3.2 Correlation between median measured *log* BCF (Cyprinus carpio) and calculated molecular polarizability 35

Figure 3.3 Predicted *log* BCF from calculated polarizability compared to measured *log* BCF... 36

Figure 3.4 Predicted *log* BCF from calculated polarizability (red diamonds), and recent (circle, triangle: based on K_{OW}, square: 3D molecular, asteroid： MCI) poly-parameter predictive methods compared to measured *log* K_{OW} for polychlorinated biphenyls. The 1:1 line (black); 1:1±0.5 line (dark grey)； 1:1±1 line (light grey) are illustrated 37

Figure 4.1 Pictures of glass plate (a) and auto squeegee (b)..... 40

Figure 4.2 GC/MS Chromatogram of SSW, SML, and PBDE Standard. The labeled peaks are listed in Table 4.1..... 43

List of Abbreviations and Symbols

ACD	Advanced Chemistry Development
BCF	Bioconcentration factor
BAF	Bioaccumulation factor
CAs	Chloroalkanes
CBs	Chlorobenzenes
CNs	Chloronaphthelenes
CTs	Chlorotoluenes
DDT	Dichlorodiphenyltrichloroethane
DSML	Dissolved Surface microlayer
EPA	U. S. Environmental Protection Agency
EPI	Estimation Programs Interface
GALAS	Global, Adjusted Locally According to Similarity
GC	Gas chromatography
GC/MS	Gas chromatography/mass spectrometry
HBCD or HBCDD	Hexabromocyclododecane
HPLC	High performance liquid chromatography
LFERs	Linear free energy relationships
LOD	Limit of detection
LOQ	Limit of quantitation
MLP	Molecular lipophilicity potential
K_{SML-W}	SML-water partition coefficient
K_{OW}	Octanol-water partitioning coefficient
OECD	Organisation for Economic Co-operation and Development

PAHs	Polycyclic aromatic hydrocarbons
PCBs	Polychlorinated biphenyls
PBDEs	Polybrominated diphenyl ethers
PFOS	Perfluorooctane sulfonate
PLSs	Partial least squares
POPs	Persistent organic pollutants
PSML	Particulate Surface microlayer
QSPR	Quantitative structure-property relationship
REACH	Registration, Evaluation, Authorisation and Restriction of Chemicals
RI	Reliability Index
RP-HPLC	Reverse Phase High Performance Liquid Chromatography
SIM	Selected Ion Monitoring
SMILES	Simplified molecular-input line-entry system
SML	Surface microlayer
SSW	Subsurface water
UNEP	United Nations Environment Programme

Chapter 1. **Introduction**

1.1. Surface Microlayer

The surface microlayer (SML) refers to the top 10-100 μm at the air-water interface (Cunliffe, 2011), and it is the boundary layer between the atmosphere and the ocean (Liss & Duce, 1997). It is physically and chemically distinct from the subsurface water below. Early descriptions of SML shows a distinct 'dry' layer containing lipid and fatty acid and 'wet' protein-polysaccharide layer; below it are bacterioneuston (the community of bacteria present within the neuston or sea surface microlayer (Franklin, et al, 2005)) and phyto-and zooneuston (microalgae and animals associated with surface water (Hardy, 1973)) (left panel in Fig. 1.1). The current model describes 'the sea-surface microlayer as a gelatinous biofilm (Sieburth, 1983), where gelatinous particles aggregate, and bacterioneuston as well as grazing protists are attached.

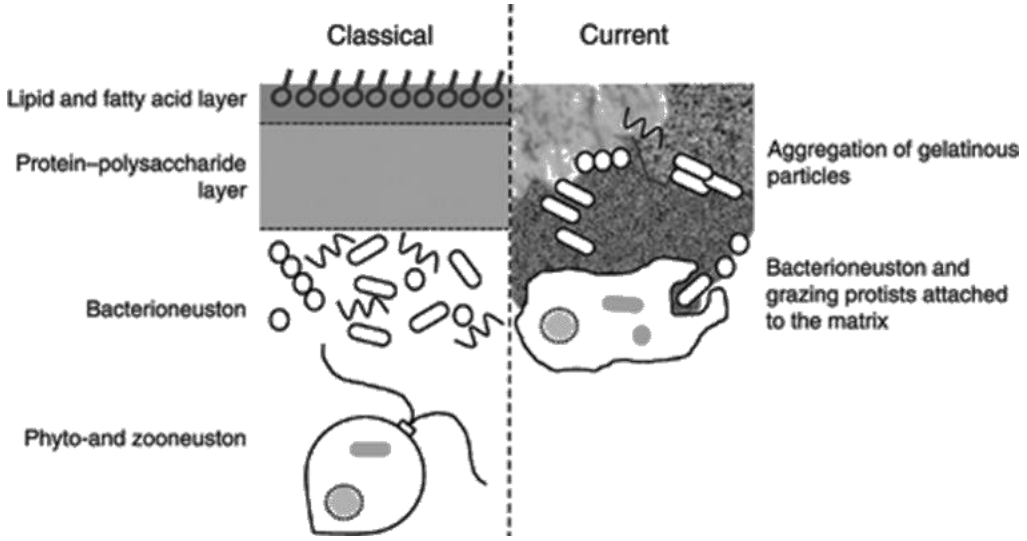

Figure 1.1 Schematic model of the structure of the air-water interface (Cunliffe, 2011)

The work of Zhang et al. (2003) showed that there was a sudden change of physical and chemical properties of the SML at the depth of 50 μm. The concentrations of dissolved trace

metals and nutrients, and some parameters closely related to organic matters in seawater were all observed to have a sharp decrease from the surface to subsurface. Naturally occurring and anthropogenic surfactants in the SML result in a decrease in the surface tension (Zitko, 2000) and a subsequent increase in the stability of the film (Zuev, 2001). It is the place where the exchanges between ocean and atmosphere happen. Therefore, properties of SML are critical to the processes of the earth ecosystem, including the synthesis, transformation and cycling of organic material, and the air–sea exchange of gases, particulate matter and aerosols.

How compounds partition into air from the water surface as well as from subsurface water (SSW) to surface is crucial to understanding persistent organic pollutants (POPs) exchange between ocean and atmosphere. SML is simplified as 'dissolved' SML (DSML) and 'particulate' SML (PSML) in studies concerning partition. However, due to the complexity of the SML, only a few studies have examined the partitioning of POPs between water and the SML, e.g. enrichment factor of total PCBs in SML relative to subsurface water was reported to vary from 0.9~62 in different sea surface microlayers (Williams and Robertson (1973), Duce et al. (1972), Abd-Allah (1999), Wurl & Obbard (2005)). It is notable that these studies only detected the DSML but neglected the PSML. According to Monodori et al.(2006), PSML enrichment is much greater than DSML, so PSML is important to consider when discussing the partitioning concerning SML.

1.2. Persistent organic pollutants

1.2.1. Definition

Persistent organic pollutants (POPs) refer to organic compounds which are persistent, bioaccumulative, subject to long-range transport and toxic. Although POPs can occur naturally, most are anthropogenic. The Stockholm Convention led by UNEP (United Nations Environment

Programme) was founded on 17 May 2004 with the aim to protect humans and the environment from adverse effects from POPs (EU, 2004). There are 27 categories of POPs classified for elimination, restriction and unintentional production in the Convention annex list and 6 in the proposed list to date (August, 2015). Polychlorinated biphenyls (PCBs), polycyclic aromatic hydrocarbons (PAHs), brominated flame retardants such as polybrominated diphenyl ethers (PBDEs), and pesticides such as dichlorodiphenyltrichloroethane (DDT) are on the annex list.

1.2.1.1. Persistent in environment

Most POPs are halogenated compounds with stable carbon-halogen bonds therefore they are resistant to chemical, biological and photolytic degradation (Ritter et al., 2007). The definition of persistence normally refers to a half-life in water of longer than 2 months and in soil and sediment longer than 6 months (Wania & Mackay, 1996) (EPA, 2012). Many POPs have been reported with an environment half-life of years, e.g. DDT 2-25 years in soil (EPA, 1989), PCBs range between 3 and 38 years in soil and sediment (Sinkkonen & Paasivirta, 2000), hexachlorbenzene 2.7-5.7 years in surface water and 5.3-11.4 years in groundwater, 0.37-1 years in sediment (Howard et al., 1991).

1.2.1.2. Bioaccumulation

Due to their hydrophobic property and resistance to degradation, POPs tend to accumulate in biotic fatty tissues and biomagnify in concentration by moving up the food chain. Bioaccumulation is the general term describing a process by which chemicals are taken up by a plant or animal either directly from exposure to a contaminated medium (soil, sediment, water) or by eating food containing the chemical (EPA, 2012).

There are two criteria that can be used to determine if a certain compound is bioaccumulative. The preferred criterion is the bioaccumulation factor (BAF) or bioconcentration factor (BCF, more detail in section 1.6) in fish (aqua), and a secondary criterion

for non-polar, hydrophobic organic chemicals is the octanol-water partition coefficient (K_{OW}, more detail in section 1.3) (Vallack, et al., 1998). BAF and/or BCF≥1000, K_{OW}≥5000 are criteria to determine if a compound is a POP. The Registration, Evaluation, Authorisation and Restriction of Chemicals (REACH) uses BCF≥1000 while Environment Canada uses both BCF and K_{OW} as criteria.

1.2.1.3. Long-range environmental transportation

Many POPs are semi-volatile with low vapour pressure (<2000 Pa). POPs with high volatility tend to remain airborne (gas phase or absorbed on particulate surface) and travel with atmospheric circulation. Those that are less volatile will partition to a condensed medium such as water, soil, and sediment. Because of the low water solubility of POPs, those found in water tend to accumulate in the SML. POPs such as organochlorine pesticides found in the ocean can travel long distances on currents (Li & Macdonald, 2005). Normally POPs half-lives with respect to atmospheric oxidation are longer than 2 days (Wania & Mackay, 1996). With their resistance to degradation and long-range transportation, POPs are globally distributed even in remote areas, e.g. PCBs were found in whole Arctic food web (Letcher, et al., 2010), For example, perfluorooctane sulfonate (PFOS) was detected in Arctic ice caps at the concentration 2.6-86 pg L^{-1} (Young, 2007), and PAHs 7.32-23.94 ng L^{-1} (mean: 13.22 ng L^{-1}) in Antarctic (Stortini et al., 2009), α-HCH (2.9 ± 0.79 ng g^{-1} dry weight) and p, p′- DDT (11 ± 3.6 ng g^{-1} dry weight) measured in over 95% of the Himalayan spruce needle samples (Wang et al., 2006).

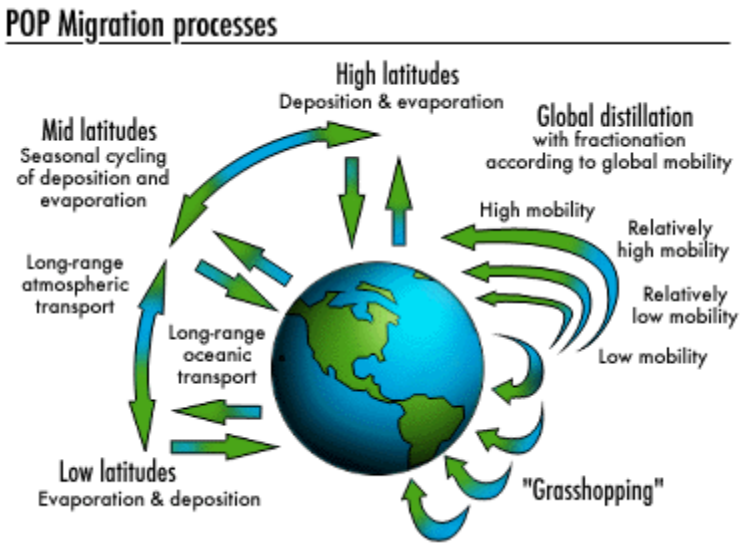

Figure 1.2 POPs Global migration Process (Wania & Mackay, 1996)

1.2.1.4. Toxicity

Various POPs have been reported to cause immune dysfunction, endocrine disruption, reproductive impairment, neural behavioural disorder and act as carcinogens (Vallack, et al., 1998). Hexabromocyclododecane (HBCD or HBCDD), a brominated flame retardant, recently added to the Stockholm Convention POPs list, was found to cause oxidative stress including acute toxicity in zebrafish embryo (Hu et al., 2009). A feeding experiment in Wistar rats showed that IgG immune response and neurobehavioral changed with the increase of HBCD concentrations in the first generation off-spring (van der Ven, 2009). Another rat experiment indicated a decrease in primordial follicle count, therefore showing that HBCD is potentially reproductively toxic (Ema et al., 2008). There have been many severe incidents of human exposure including dioxin pollution in chicken (Belgium, 1995), egg (German, 2005), cheese (Italy, 2008), pork (Ireland, 2008), and fodder (German, 2011). Knowledge of the physical properties of POPs, such as partition coefficients, is critical to understand and predict their toxicity, long-range transport, deposition and elimination in the environment.

1.2.2. POPs present in SML

As mentioned in section 1.2.1.3, POPs in SML plays an important role in understanding global transportation, how POPs partition into SML from water and then move into air becomes a vital unsolved problem. In this thesis, we define the partition property of compounds between SML and water as the SML-water partition coefficient (K_{SML-W}). As an organic compound-enriched condensed phase, we look at the K_{OW} and BCF of a compound as proxies for the K_{SML-W}, as both characterize partition properties between a condensed, organic-like matter (octanol, organism) and water. This would represent the primary properties of concern when studying the partition properties regarding the SML environment.

1.3. Octanol–water partition coefficient

Octanol–water partition coefficient (K_{OW}) represents the ratio of the solubility of a compound in octanol to its solubility in water (EPA, 2012). It is assumed that the molecular speciation of the chemical is the same in octanol and water, and that the solutions are sufficiently diluted (Sangster, 1997), i.e. when the system reaches equilibrium at a specified temperature,

$$K_{OW} = \frac{c_{octanol}}{c_{water}}. \qquad (1.1)$$

K_{OW} is an important physical property of a chemical, which is recognised as of equal importance as vapour pressure, water solubility and toxicity by EPA and OECD (Organisation for Economic Co-operation and Development). The carbon/oxygen ratio (8:1) in octanol is similar to that in organisms or parts of organisms, including biota and natural organic matter. Therefore, the octanol-water partitioning system mimics the lipid membrane-water system, and K_{OW} can be a good indicator of the chemical's ability to partition in the environment between water and natural solids (such as soil, sediment, and suspended particles) or organisms (such as fish, mammals, and microorganisms) (Schwarzenbach et al., 2004).

1.3.1. Experimental methods used to determine K_{OW}

1.3.1.1. Flask shaking method

The shake flask method is a direct method to determine K_{OW}. It involves preparing a compound with known concentration in one phase (octanol or water) in a flask, then mixing it with the other phase, shaking the flask vigorously, and allowing the two phases totally separated by which the system will eventually reach an equilibrium state (Sangster, 1989). K_{OW} is obtained using eq. (1.1) when the concentrations of the compound in both phases ideally are measured. The temperature should be kept between 20°C and 25°C with a maximum variation of ± 1°C (OECD, 1995). In the experiment, only the concentration in one phase will be measured, while concentration in the other phase is calculated using mass conservation, assuming the chemical is not absorbed on the surface of glassware or other surfaces. The shake flask method is the most traditional and widely-used method using easily accessible instruments, and applicable to compounds with *log* K_{OW} ranged from 2 to 4 (OECD, 1995). However, this method ignores the fact that octanol and water are not exclusively immiscible. The octanol phase will contain 20% water and the water phase will contain $8*10^{-3}$ % octanol under equilibrium condition (Schwarzenbach et al., 2004), leading to formation of microdroplets. Measuring the concentration under some situations can be very difficult, e.g. when a compound is extremely hydrophobic or hydrophilic, the concentration in the relevant phases will be exceedingly small, and thus difficult to quantify.

1.3.1.2. Generator Column Method

The generator column method involves generating a water-based solution by pumping water into a column which is saturated with a fixed concentration (normally 0.1% w/w) in octanol. The water phase with partitioned test chemical is eluted. Then the water phase which passes through an extractor column, is ultimately analyzed, typically using chromatography

techniques (OECD, 2002). This is also a direct method and very versatile, applicable to chemicals with *log* K_{OW}>1 at 25 ℃. The advantage of this method compared to the shake flask method is that it avoids two phases mixing, while the disadvantage is the usage of more sophisticated instrument which is specially designed for this method.

1.3.1.3. Slow stirring method

The slow stirring method is similar to the shake-flask method, but it reduces the microdroplet formation by equilibrating octanol, water and the test compounds in a thermostatic stirred reactor (OECD, Test 123 Partition Coefficient (1-Octanol/Water): Slow-Stirring Method, 2006), so it is particularly suitable for substance with *log* K_{OW} 5~8.3 (Tolls, et al., 2003). The experiment is operated under 25 ℃±1 ℃. The octanol phase is slowly piped onto the wall of reaction vessel to avoid turbulence and hence a film is formed above the water phase (OECD, 2006). But the slow stirring method also does not perform well when considering highly hydrophobic or hydrophilic compounds.

1.3.1.4. Chromatography

High-performance liquid chromatography (HPLC) can also be used to obtain K_{OW}. The methods involve using a series of compounds with known K_{OW} as standards. The K_{OW} can be determined by correlating the retention time of a compound to those of known standards. The principle of this method is that the chemical injected on C8, C18 column partitions between the mobile solvent phase and the hydrocarbon stationary phase. The retention time shows the ability of their hydrocarbon-water partition coefficients, from which partition between octanol and water can be computed (OECD, 2004). It's a fast method, and it commonly takes 5~20 minutes per sample. But it is limited to those of similar chemical structure and extrapolations to other chemical classes are not applicable (Valkó, 2004). RP-HPLC (Reverse Phase HPLC) method works for K_{OW} between 0 and 6, but can be expanded to 6-10 if the mobile phase is modified

(OECD, 2004). Griffin et al. (1999) measured K_{OW} for 57 terpenoids using RP- HPLC with 6 non-phenolic and 3 phenolic standards. The results gave a good correlation with the shake flasks method with consistent precision over the *log* K_{OW} range of 1.8~4.5.

1.3.2. Computational methods

Although data from experimental methods are generally considered to be most reliable, high operation requirements and quality issues (as described above) limit their utility. Therefore, experimental data is sometimes not complete, unreliable, or incomparable. With inexpensive, rapid computation technology, predictive models based on molecular structures to estimate partition coefficient K_{OW} has become popular.

The quantitative structure-property relationship (QSPR), based on the assumption that similar molecular structures have similar properties, establishes correlations between physical properties and molecular descriptors of a compound. The logarithm of the equilibrium constant is expressed as a linear function of variables which describe the relevant interaction energies (linear free energy relationships (LFERs) (Wells, 1963)). Molecular descriptors can be collected from different sources such as substituent constants, physicochemical properties, quantum chemical calculations and the theoretical structural parameters derived from one or two dimensional molecular structures. A large number of molecular descriptors (training set) are randomly selected as arguments for statistical methods, such as partial least squares (PLSs), non-linear/linear regressions and artificial neural network to develop the prediction model. An external set of validation data is used to evaluate the result of the model.

Numerous QSAR models using different molecular descriptors have been developed to predict K_{OW}. Generally, these models can be classified into 2 main categories: substructure approaches and whole molecule approaches (Mannholda & van de Waterbeemd, 2001).

1.3.2.1. Substructure approaches

Substructure approaches assume that each atom or fragment has contribution to *log* K_{OW}, and these contributions are additive. The basic strategy of these methods is first breaking a target molecule down to atoms or fragments, and then modelling the contribution with available experiment data with regression methods. In many models developed to calculate K_{OW} using substructure approaches, ClogP, ACD logP and EPI suite are the three most matured and widely employed approaches. They all accept easy SMILES (Simplified Molecular-Input Line-Entry System) input, built on the basis of similar database size of about 13,000 compounds.

ACD logP

ACD (Advanced Chemistry Development) logP follows a pure fragmental method developed by Hansch and Leo (1979). Its calculation procedure contains two steps: fundamental fragmental values are first derived from small molecules with available experimental data and the remaining fragment set is constructed, then a correction value associated with factors such as bonds and branching is applied. ACD logP incorporates two different predictive approaches, Classic and GALAS. The Classic approach uses fragmental logP contributions derived from atoms, structural fragments and intramolecular interactions (van der Waals interactions and H-bonds for non-ionic organic compounds) experimental logP values as primary algorithm and a secondary algorithm applied when unknown fragments are present in the molecule. GALAS (Global, Adjusted Locally According to Similarity) provides a quantitative estimate of reliability of prediction through the Reliability Index (RI). Besides, ACD logP features the ability for the user to employ custom experimental data in the expansion of the Applicability Domain as a corresponding prediction method (Machatha & Yalkowsky, 2005). ACD logP calculation is simple and it can distinguish tautomeric forms and its striking feature is usage of large numbers of increments for aromatic interactions (Mannholda & van de Waterbeemd, 2001).

EPI Suite

The EPI (Estimation Programs Interface) Suite is a series of free models developed by EPA and Syracuse Research Corp (EPA, 2012). It can estimate different physical/chemical properties and environmental fate in Windows interface. KOWWIN and WSKOWWIN are used to calculate K_{OW} in EPI Suite. This method was first introduced as an atom/fragment method by Meylan and Howard (1995). The overall strategy includes two steps: correlation atom/fragment with *log* K_{OW} contribution and then correlation with correction factors. KOWWIN employs 508 fragment counts and correction factors (both used as descriptors) derived from experimental K_{OW} values, while WSKOWWI uses a chemical's water solubility as applicable correction factor, if any, from the value obtained from KOWWIN. The advantage of this program is its free access and universal application including stereo-chemical isomers. The cons are its relatively large error of prediction and slow calculations concerning zwitterionic molecules.

CLOGP

The CLOGP program is also designed on the conception of Hansch and Leo (1979) and is now commercially available from Pomona College and BioByte, Inc. of Claremont, CA. CLOGP is different from ACD log P in that H-atoms are detached from isolated carbons in CLOGP; and CLOGP uses the type of functional group and the length of the alkyl chain as branching correction factors to improve the accuracy (Petrauskas & Kolovanov, 2000). The high accuracy of CLOGP makes it (with error lower than ACD logP and EPI suite (Mannhold & Petrauskas, 2003) (Machatha & Yalkowsky, 2005)) the most commonly used *log* K_{OW} calculation program. Its drawbacks are its deficiency in distinguishing enantiomers and the sophisticated computer configuration required when a complex compound is investigated.

1.3.2.2. Whole molecule approach

The whole molecule approach considers the target molecule as a whole, and uses charge densities, surface area, topological indices (MLOGP (Moriguchi et al., 1992), AUTOLOGP (Devillers et al., 1998)), 3-D structure including implicit solvation, and molecular hydrophobicity potentials (CLIP (Gailard et al.,1994)) as descriptors to determine *log* K_{OW} with regression methods. Most whole molecule models are computationally intense considering the fact that more and more new descriptors are being discovered and included into algorithms. Molecular lipophilicity potential (MLP) describes the hydrophobic potential of the fragments in a molecule; therefore, it denotes the strength of intermolecular interactions between a compound and octanol-water system. MLP was first introduced by Audry et al. (1986) as a structure-activity predictor. Topological indices are graph invariant numbers calculated based on the molecular graph of a chemical (Hendrik et al., 2002). It contains numerical values associated with chemical constitutes related to chemical structure (Babujee, 2012).

Various quantum chemical descriptors, such as molecular size (Bodor & Buchwald, 1997), surface area and the electrostatic potential (Haeberlein & Brinck, 1997), volume, surface, shape and dipole moment (Bodor et al., 1989), charge distribution, super delocalization ability (Bodor & Huang, 1992), molecular weight and heat of formation have been related to *log* K_{OW}. Water solubility (Bowman & Sans, 1983) is also reported to be able to predict K_{OW}.

Whole molecule approaches do not necessarily have only one descriptor; most models use two or more descriptors to obtain the best results on a strictly statistical basis. Zhou et al. (2005) optimized the number and combination of candidate molecular descriptors by judging the resultant predictions statistically, determining which of the many molecular descriptors chosen yield the best predictive power (e.g. (Zhou, Zhai, Wang, & Wang, 2005)). In general, poly-parameter methods do perform very well, as judged by the coefficient of determination and slope

of the comparison between measured and predicted values. However, it is important to remember that through increasing the number of descriptors in the predictive method, the coefficient of determination in a multi-parameter regression will almost always increases, even if the descriptor has no effect., for example, the prediction power of a model to predict K_{OW} of PCBs (Yu et al.,2016) increased by adding atomic number (to distinguish atom types) as a second parameter other than number of hydrogen atoms. In fact, these two parameters are not exclusive. Although such approaches often yield excellent results, these are generally not transferrable beyond the class of compound used in the statistical fit procedure. Further, there is no general prescription, other than statistical success, for choosing which of the molecular descriptions to include in the relationship. Besides, these models may still need input of experimental parameters, although they perform well considering error and relevant coefficient.

1.4. Bioconcentration factor

Bioconcentration is the process representing a net accumulation of a chemical directly from an exposure medium (e.g. fish in water, microorganism in water) into an organism (EPA, 2012). Bioconcentration only relates to respiratory and dermal surface, not to diet uptake. It is the net result of competing rates of chemical uptake at the respiratory surface (k_1, L kg^{-1} d^{-1}) and chemical elimination (k_2,) including respiratory exchange (k_2, d^{-1}), fecal egestion (k_E, d^{-1}), metabolic biotransformation (k_M, d^{-1}) and growth dilution (k_G, d^{-1}). Bioconcentration factor is a term which expresses the degree of concentration. As discussed in 1.1, the partition concerning SML, i.e. gelatinous particles with bacterioneuston and grazing protists, may greatly attribute to the BCF property.

1.4.1. Experimental methods

Based on the bioconcentration definition, BCF can only be measured under lab conditions, in which the diet uptake can be strictly excluded (Arnot & Gobas, 2006). If an organism is considered to be a single compartment in a homogeneous medium, the bioconcentration can be expressed as

$$\frac{dC_B}{dt} = k_1 C_{WD} - (k_2 + k_E + k_M + k_G) C_B, \qquad (1.2)$$

where C_B (g /kg) is the chemical concentration, it is a function of time t (days), and the free dissolved chemical concentration of the organism in water is denoted as C_{WD}, (g/L). When the system reaches a steady state, C_B and C_{WD} no longer change with exposure time, i.e. $\frac{dC_B}{dt} = 0$, eq. 1.2 can be rearranged as

$$\mathrm{BCF} = \frac{C_B}{C_{WD}} \qquad (1.3)$$

$$= \frac{k_1}{k_2 + k_E + k_M + k_G} = \frac{k_1}{k_{2'}} \qquad (1.4)$$

The flow-through fish method (OECD, 1996) is based on eq. 1.3 and eq. 1.4. This method is most validly applied to stable organic chemicals with *log* K_{OW} values between 1.5 and 6.0 (Hawker & Connell, 1988), but may still be applied to superhydrophobic substances (*log* $K_{OW} > 6.0$). To simplify, this method involves the exposure (uptake) and post-exposure (depuration) phases. In the exposure phase, separate groups of fish are kept in tanks with different chemical concentrations (at least 2 concentrations and 1 blank as the control group) for equilibrium (steady-state) or 60 days if equilibrium is not reached earlier. In the post-exposure phase, the fish are transferred to clean tanks without tested chemical and kept until appropriate reduction (e.g. 95%) of the tested chemical in the body occurs. k_1, $k_{2'}$ can be derived from uptake and depuration curve. Then the steady-state BCF_{SS} can be therefore expressed as

$$BCF_{ss} = \frac{C_B \text{ at steady state}}{C_{WD} \text{ at steady state}} \qquad (1.5)$$

$$\text{BCF} = \frac{k_1}{k_{2'}} \qquad (1.6)$$

The steady-state method is only valid when a steady state actually occurs, but can be used for hazard assessment in a near "steady-state" at 80% ($1.6/k_{2'}$) or 95% ($3.0/k_{2'}$) of equilibrium (OECD, 1996).

1.4.2. Computational Methods

The considerable cost and time for a fish bioconcentration test, especially when it requires the use of radiolabelled chemicals, urges the development of new calculation methods for BCF. However, a limited number of models have been developed to predict BCF due to a lack of data and relatively higher complexity of BCF compared to K_{OW}. Therefore, different models have been developed to predict BCF using K_{OW}, e.g. linear (Veith et al., 1979; Macek et al., 1980; Mackay, 1982; Isnard &Lambert, 1988), polynomial (Southworth et al., 1980), bilinear (Connell & Hawker, 1988) and base-line model (Dimitrov, 2005). Harald et al. (1991) successfully correlated the *log* BCF for selected chemicals in algae, mussels and daphnia using K_{OW}-based linear regression analysis. This study gives a compilation of BCF on a wet weight basis (BCF_w) of 52 organic chemicals by the three organisms from aqueous solution; BAFBCF in EPI suite is also built on this principle, BAFBCF employs proper correction factors to achieve a better prediction power.

Another approach to estimate BCF is based on the food web bioaccumulation model, which was first proposed by Hamelink et al. (1971). The food web model considers absorption and solubility differences as the principle parameters. It calculates BCF using eq. 1.2. Many researchers have improved the model. A significant improvement by Arnot and Gobas (2004), incorporates the mechanism of bioaccumulation derived from laboratory experiments, field

studies and improvements in model parameterization to provide better estimates of BCF in comparison to the previous food web model without largely changing input requirements. The second method in BCFBAF calculates BCF from mechanistic first principles using the Arnot-Gobas method and estimates BCF and BAF at three trophic levels.

Recognizing the significance of different mitigating factors associated either with interactions or with an organism or bioavailability, Dimitrov et al. (2005) proposed a base-line model for *log* BCF, using a simulator for fish liver with a training set of 511 chemicals. The chemical structure as well as metabolism is taken into account in the model.

Another free QSAR model, CAESAR (Zhao et al., 2008) is a neural network based on 8 descriptors calculated from third-party software using a dataset of 473 compounds with experimentally-determined BCF. This model provides a quantitative prediction of BCF in fish with an error within 0.5 *log* unit. The model reached an $R^2 = 0.83$ on the training set, and $R^2 = 0.80$ on the validation set. A more advanced version of CAESAR, VEGA integrates a software which optimizes choice of descriptors; thus, only needs the input of molecular structure. This model gave better results than BCFBAF v3.00 for the chemicals in the applicability domain of the model (Lombardo et al., 2010). Isomers cannot be distinguished in this model.

1.5. SML sampling method

The properties of the SML, as well as weather conditions, such as wind, wave, and temperature, raise difficulties in sampling SML. Several sampling methods have been developed using different techniques.

1.5.1. Plate sampler

The glass plate method, which involves immersing a clean, hydrophilic glass plate vertically into the water and slowly pulling out at a controlled rate, then using a squeegee or

wiper blade to scrub the SML sample from both sides of glass plate surface. This is the most widely used sampling method. This technique was originally introduced by Harvey and Burzell (1972) as shown in Fig.1.4. Most recent techniques use a plastic handle fixed on the top of glass for convenience.

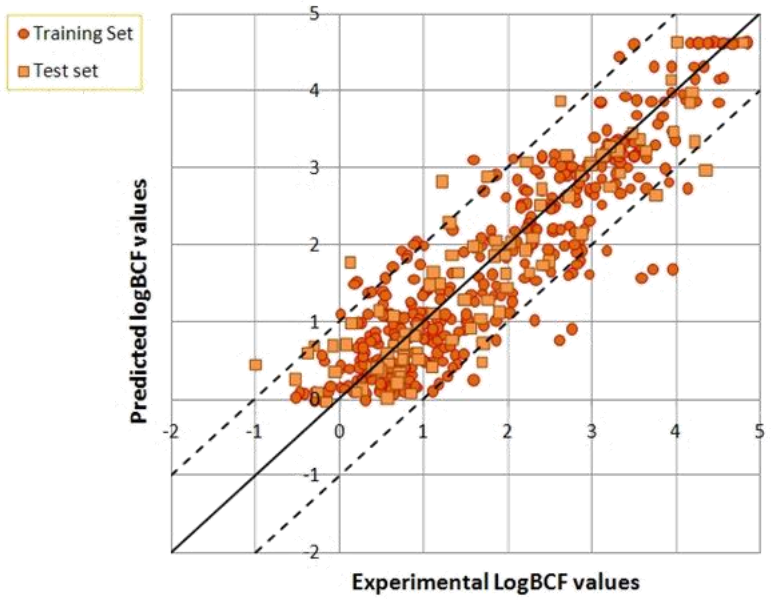

Figure 1.3 The predicted and experimental log BCF values obtained with the CAESAR model (Adopted from CAESAR (2006) without permission)

A layer of approximately 60~100 μm depth can be retained based on the different withdraw rates. A Teflon plate can be also used which collects 10 μm-thick samples (Falkowska, 1999). With different properties, water samples from Teflon plates contain non-polar substances while those from glass plate contain weakly polar compounds of hydrocarbon origin, their strongly polar derivatives, and very small living organisms. The glass plate method is most accessible and very economical; it can perform well even under difficult weather conditions (Falkowska, 1999). However, sampling with a plate can be time-consuming and labour intensive.

Some 60 samplings with glass plate and about 1000 samplings with Teflon plate (both 30*30 cm size) at withdrawal rate of 5~6 cm s^{-1} were needed to obtain 1 dm^3 SML from ocean water.

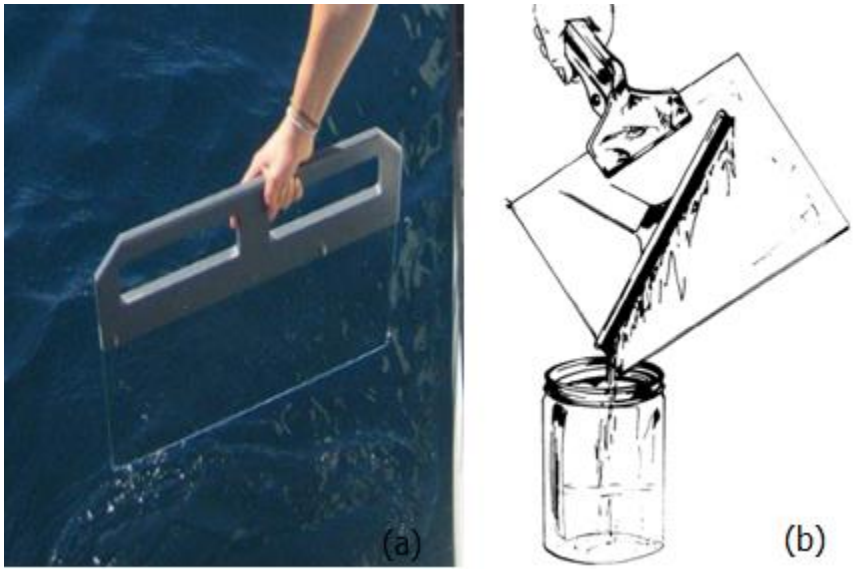

Figure 1.4 Glass plate sampler. (a) shows the glass plate sampler (reproduced from Van Pinxteren et al., 2012) while (b) illustrates removal of microlayer, reproduced from Harvey & Burzell (2003).

1.5.2. Mesh screen and membrane surface methods

The mesh screen method is another common sampling method. A metal screen mesh frame is contacted with the water surface, then vertically withdrawn. The sampled water is drained into collection bottles. The mesh is typically made of 0.2mm~0.3mm diameter stainless steel metal wire, which is close to the thickness of the surface layer. The variability of mesh size can decrease robustness of this method. The membrane filter method, built on the similar conception, uses a membrane filter to obtain the very top layer ($\leq$ 40 μm) of the water. This is the most labour-intensive sampling method, due to the small surface of membrane. However, it gives the best performance when studying the very top surface.

1.5.3. Rotating drum method

A more advanced sampling method involving a floating boat and a rotating drum (cylinder) (Fig. 1.5) was first constructed by Harvey (1966). The surface water was entrained

while the drum was rotating on the water surface, and then continuously removed off by a large blade tightly fixed onto the drum into a collection jar. The instrument can operate continuously at a controlled rate and it only causes slight turbulence on a slow-pushing boat. By adjusting the rotating speed, approximately 60 μm thickness surface layer can be sampled. The instrumentation is autonomous which saves time and labour, vertical mixing is reduced during the sampling process so as to lessen sample contamination. The limitation is that it can only be used under calm conditions in large open water areas. A very large device is needed to overcome the difficulty in rough water.

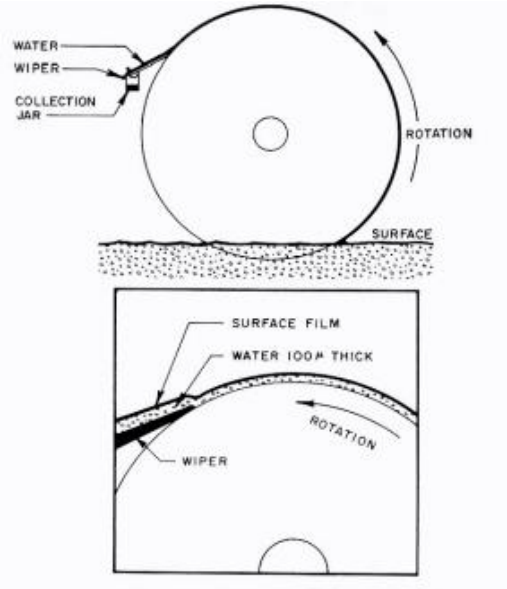

Figure 1.5 Rotating drum method for sampling SML, reproduced from Harvey (2003).

1.5.4. Rotating glass disk method

The rotating glass disk method is a hybrid technique combining a set of glass plates and the rotating drum method developed by Shinki et al. (2012). The instrument is shown in fig.1.6. A set of glass disks with Teflon wipes in between are mounted with appropriate intervals to avoid disk-disk interference. The instrument is equipped with a GPS receiver, a fluorescence

spectral meter and a weather station. It can be remotely controlled within 3 km. The rotating disk instrumentation spins faster than a conventional drum sampler; because it decreases the contact area with water surface, the instrument can be operated in bad sea conditions with minimal disruption of water surface. Each of the glass plates is replaceable and works in parallel with each other when collecting surface water samples within the top 60 μm in the surface layer.

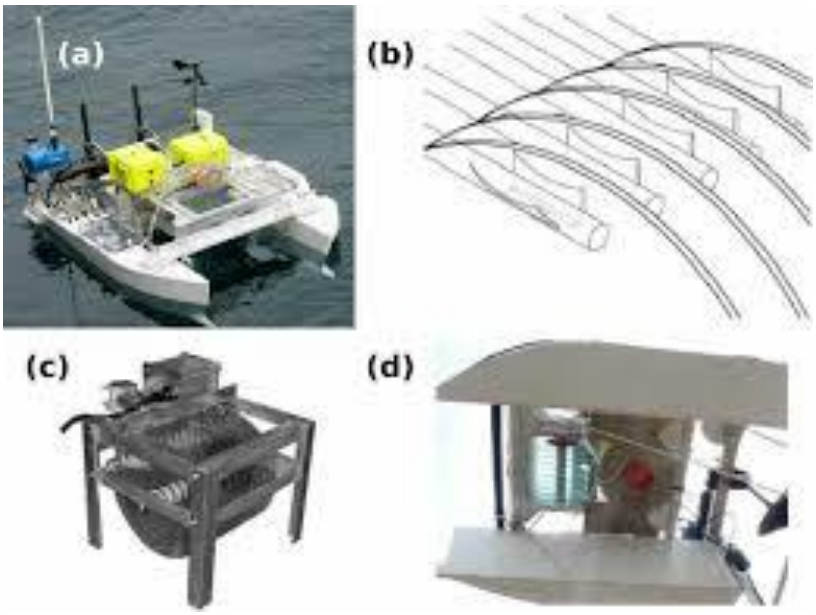

Figure 1.6 (a) Photograph of a rotating disk microlayer sampler. (b) Schematic diagram showing glass disks with Teflon wipers in between. (c) The glass disk module. (d) Bottom view of the vessel, indicating the location of the glass-disk module, adapted without permission from Shinki et al. 2012.

Many factors influence the thickness of collected sample including wind speed, air and water temperature, withdrawal or rotation speed, salinity and the content of surfactants. The fact is that different instruments/methods yield different actual sampling depths, which means the biological and chemical compositions will be different; hence, the research results from different methods are not comparable. The chemist can choose from available instrumentation and objectives based on pros and cons.

1.6. Objectives

The objectives of this research are to find a suitable parameter to predict the partition coefficient of a persistent organic pollutant concerning surface microlayer and subsurface microlayer. Since octanol can be seen a surrogate of biota and naturally occurred organic matter and SML is constituted of both, parameters that predict *log* K_{OW} could also be a good indicator of *log* K_{SML-W}. Similarly, improved prediction of BCF could aid in our understanding of partitioning between water and the SML. Polarizability will be examined as a potential single-parameter predictor of both *log* K_{OW} (Chapter 2) and BCF (Chapter 3). Testing the applicability of polarizability to *log* K_{SML-W} requires the robust measurement of POPs in both sub-surface water and the SML. A new, efficient, SML sampling method will be developed and used to collect samples for POPs analysis (Chapter 4). This work will improve our understanding of the factors driving partitioning between water and the SML.

Chapter 2. **Molecular polarizability as a single parameter to predict Octanol-water partition coefficient**

2.1. Introduction

Knowledge of physical properties is critical to understanding and predicting the environmental disposition and transport of persistent chemicals. Partitioning coefficients can be extremely difficult to measure for some chemical species, such as POPs, due to their low solubility in one or both phases and a lack of available pure standards. As a result, measured partitioning coefficients for POPs often have large uncertainties and inter-experimental differences can be an order of magnitude or greater (Wania & Mackay, 1996). Because of the difficulties in acquiring accurate and precise experimental measurements, predictive methods have proved very useful in the determination of physical properties for POPs. Numerous models exist to predict the partitioning properties of POPs (e.g. Chiou et al., 2005; Whittekindt & Goss, 2009), but many require the use of empirical chemical properties. These can be difficult to obtain, for similar reasons as those which plague direct partitioning measurements. As a result, *a-priori* predictive models that can be used without the input of experimental data are useful in determining partitioning properties of POPs.

Given that partitioning properties are ultimately the result of inter-molecular interactions, one may consider starting afresh, using a thermodynamic approach to justify a fixed set of input molecular parameters. Partitioning coefficients are a measure of the relative inter-molecular interactions between a target compound and the two phases under consideration. For non-polar compounds, which do not participate in specific (i.e. hydrogen bonding) interactions with the solvent, inter-molecular interactions arise from transient charge distributions induced by local electric fields, such as those caused by the neighbouring molecules that compose the bulk phase.

For molecules that interact primarily via dispersion interactions, these transient charges depend on the molecular polarizability of the target compound, which describes the ability of a molecule to acquire a dipole moment in the presence of an electric field. As such, molecular polarizability could be an effective property with which to predict partitioning coefficients, as it can be directly and accurately calculated using quantum mechanical modeling (Hickey & Rowley, 2014). Previous studies demonstrated that molecular polarizability calculated using quantum mechanical methods can describe variability in, and effectively predict, the subcooled vapour pressure and octanol-air partitioning coefficient of chlorinated POPs (Staikova et al., 2004; Staikova et al., 2005).

K_{OW} is widely used in environmental models to predict the fate of POPs in the environment (e.g. Mackay et al., 1996; Connell et al., 1998). It is an important input parameter to equilibrium-based partitioning models which estimate partitioning coefficients such as bioconcentration (Walters et al., 2011). Measurements of K_{OW} are challenging, particularly for very hydrophobic POPs, where, for example, emulsified octanol within the aqueous phase can lead to erroneously low K_{OW} values. Variability in reported K_{OW} can lead to significant inaccuracies in assessments of risk and remediation (Linkov et al., 2009). As a result, it is important that K_{OW} values be known accurately. Here, we demonstrate the ability of calculated molecular polarizability to both describe the variability in and act as the sole predictive property for octanol-water partitioning coefficients.

2.2. Methods

Previous studies (e.g. Staikova et al., 2005; Staikova et al., 2004) reported the results of quantum mechanical calculations of the polarizabilities of 167 chlorinated POPs in several classes, consisting of 12 chlorobenzenes (CBs), 11 chlorotoluenes (CTs), 26 chloronaphthelenes

(CNs), 39 chloroalkanes (CAs), 69 PCBs, 4 chlorinated pesticides, as well as hydrogenated analogues of each chemical class. Gaussian 98 (Frisch, et al., 1998) was used to calculate the optimized geometries and molecular polarizabilities using density functional theory with B3LYP functionals and the 6-311g(d,p) basis set. We calculated the polarizability of 119 additional compounds: 23 fluoroalkanes, 10 fluorobenzenes, 52 brominated compounds, and 34 mixed halogenated compounds using the same functionals with Gaussian 09 (shown in Fig. S.1). The polarizability was calculated as the arithmetic average of the x, y, and z components:

$$\alpha_m = (\alpha_{xx} + \alpha_{yy} + \alpha_{zz})/3$$

A full list of compounds and their calculated polarizability values including those reproduced from Staikova et al. (2005) and Staikova et al. (2004) are shown in Table S.2.

Experimentally measured K_{OW} values were available for 127 of the 286 hydrocarbon, chlorinated fluorinated, and brominated species that were included here. Experimental values were taken from Mackay et al. (2006) and references therein. Reported values determined using estimation methods, such as chromatographic retention time, were not included among the 127 to ensure that bias arising from assumptions implicit in those estimates did not influence the results of this work. Among the 127 compounds for which measured K_{OW} data existed, 95 (~three quarters) were randomly selected to form a training set, while the remaining 33 compounds (~one quarter) made up the validation set. Compounds from every sub-class were included in both the training and validation sets. To derive the predictive relationship, a linear least-squares regression was used to relate the mean (where available) measured *log* K_{OW} to calculated molecular polarizability. The regression was weighted by the standard error of mean measurements. For compounds with a single *log* K_{OW} measurement, an error equivalent to the maximum standard error of the mean within the training set compounds was used.

2.3. Thermodynamic Premise

The octanol-water partitioning coefficient, K_{OW}, for a compound is determined experimentally from the ratio of its equilibrium concentrations in the two phases; thus, it depends upon its relative solubility in each phase. At equilibrium, the ratio of a compound's chemical activity in the octanol phase to that in water gives a thermodynamic equilibrium constant, which is related to the standard Gibbs energy of phase transfer:

$$logK_{ow,x} = \frac{-\Delta G^{o}_{ow,x}}{2.303RT} \quad (2.1).$$

$\Delta G^{0}_{ow,x}$ gives the Gibbs energy difference between an octanol solution of *x* in its standard state and an aqueous solution in the standard state.

In his classic text, Isrealachvili (1992) defines the free energy of transfer of compound "*x*" from solvent "*A*" to solvent "*B*", in the case where only dispersion forces operate (ΔG_{BA}^{disp}). Given a solvation shell of 12 solvent molecules, the transfer can be thought of as requiring the removal (desolvation) of solute *x* from the cavity formed by *A* and the consequent re-formation of 6 *A*-*A* bonds, and the creation of a cavity in *B* (breaking 6 *B*-*B* bonds) followed by the solvation of *x* in this cavity. Assuming (for simplicity) that all the molecular sizes (σ) are comparable and have similar ionization energies (given by $h\nu_I$), the simple result may be written:

$$\Delta G_{BA}^{disp} \approx \frac{3h\upsilon_1}{4\sigma^6(4\pi\varepsilon_0)^2}[-(6\alpha_A^2 - 12\alpha_x\alpha_A) + (6\alpha_B^2 - 12\alpha_x\alpha_B)] \quad (2.2),$$

where α represents the zero-order, static polarizabilities of the indicated species. By rearranging, the following can be obtained:

$$\Delta G_{BA}^{disp} \approx \frac{3h\upsilon_1}{4\sigma^6(4\pi\varepsilon_0)^2}[6(\alpha_B^2 - \alpha_A^2) + 12\alpha_x(\alpha_A - \alpha_B)] \quad (2.3),$$

which suggests that ΔG_{BA}^{disp} (and therefore *log* K_{BA}) is a linear function of α_x.

We expect that dispersion forces will dominate the solvation of our test compounds in the octanol phase. In the water phase, water-water interactions will be complex, involving hydrogen bonding and dipolar interactions as well as dispersion forces. However, such water-water interactions are only of importance in the cavity re-formation energy term, and do not affect the dependence of the Gibbs energy of transfer on solute properties. Given our selection of solutes, which are not expected to enter into specific interactions with water, there are no solute-water hydrogen bonding terms to consider, but there may be an additional dipole-induced dipole interaction between the 12 solvent water molecules and the solute. Such interaction energies will have the form:

$$E_{interact} \approx -12 \frac{\mu^2{}_W \alpha_x}{(4\pi\varepsilon_0)^2 \sigma^6} \quad (2.4)$$

and so will merely add a constant term to the slope of a *log* K_{OW} vs. α_x plot. We note that this argument assumes the entropic contribution to the free energy of transfer is not strongly solute-dependent.

2.4. Results and Discussion

The results shown in Fig. 2.1 display the excellent correlation ($r^2 = 0.92$) between measured median *log* K_{OW} values and calculated polarizability for all 286 chlorinated, fluorinated, and brominated POPs for which measurements exist. The large value of the correlation coefficient indicates a strong relationship exists between the molecular polarizability and *log* K_{OW}, as postulated above. One striking and clear advantage of this model is its ability to resolve differences between measured *log* K_{OW} for structural isomers, as illustrated by the red symbols in Fig. 2.1. We note that molecular weight, molecular volume, and number of electrons have all been used in LFERs that seek to predict environmentally-important parameters. Each of

these attributes can be thought of as a proxy for molecular polarizability. A relationship based on molecular weight or number of electrons is not able to distinguish between structural isomers, or similarly-massed compounds.

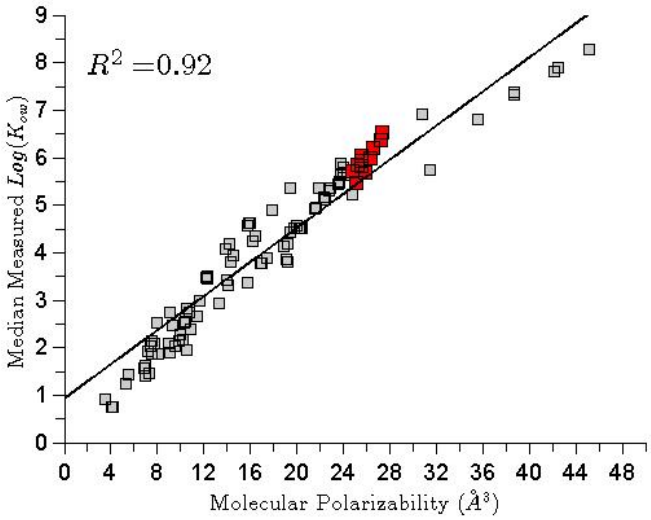

Figure 2.1 Correlation between median measured log K_{OW} (from Reference 1 and references therein) and calculated molecular polarizability. Red squares indicate 11 tetrachlorobiphenyl isomers; a linear regression through all data is shown by the black line.

A predictive model for *log* K_{OW} using calculated polarizability was developed using the data described above. 95 halogenated POPs were randomly selected to form a training set, ensuring that at least one chemical each of CBs, CTs, CNs, CAs, PCBs, chlorinated pesticides, hydrogenated analogues, fluoroalkenes, fluorobenzenes, bromogenated and mixed halogenated compounds was included. The predictive relationship derived from the regression:

$$log\ K_{OW} = (0.165 \pm 0.009)\alpha + (1.1 \pm 0.2) \qquad (2.5)$$

was used to predict the octanol-water partitioning coefficient for the remaining 32 compounds. A comparison between predicted and measured *log* K_{OW} for all chemicals with measurement data is shown in Fig. 2.2. The relationship is able to predict all compounds in the validation set to within one *log* unit of the measured mean *log* K_{OW} value. Predicted *log* K_{OW} values for 83% and 58% of the training set compounds were within 0.50 and 0.25 *log* units, respectively, of the measured

mean *log* K_{OW} values. Considering the variability in measured values from experimental method is typically larger than 0.1 *log* unit (Mackay et al., 2006), the correlation described here is excellent. The predictive method can easily be applied to compounds for which measurements are limited or non-existent. Predicted *log* K_{OW} values for all 286 compounds can be found in the Table S.2.

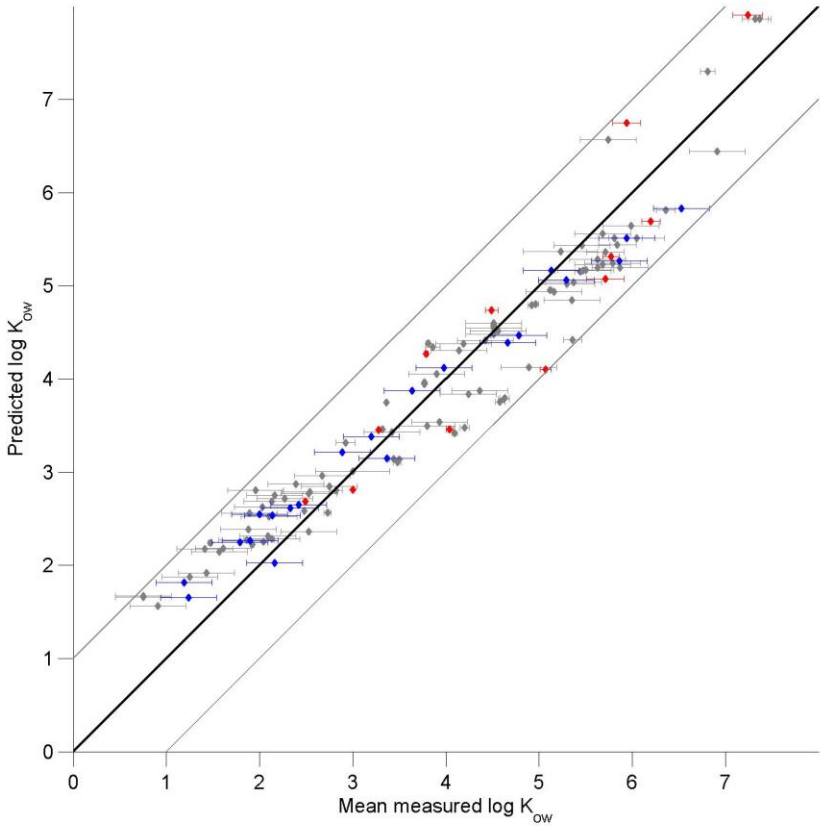

Figure 2.2 Predicted log K_{OW} from calculated polarizability compared to measured log K_{OW} for 286 compounds. The training set (n=95) is shown in grey, the 1:1 line (black) and 1:1 line ± 1 log unit (grey) are shown as well. The validation set (n=33) is shown as red and blue symbols, where the red symbols display the mean ± standard error when there are several measurements, and the blue shows the cases of a single measurement ± its assumed error range.

Numerous predictive methods exist in the literature for the *log* K_{OW} of chlorinated persistent pollutants (e.g. Zhang et al., 2013; Zhou et al., 2005; Wu et al., 2002); Some of them predict values close to the measured values (i.e. within 0.3 *log* units). In order to obtain these

high correlations coefficients, as many as 18 independent parameters (Zhang et al., 2013) have been used. It has been previously noted that using statistical methods and multiple parameters to develop a LFER can lead to chance correlations without real physical meaning (Hansen et al., 1999). Furthermore, correlation coefficients, if not adjusted for the number of parameters included in the regression, will be higher than is justified by the predictive power of the variables.

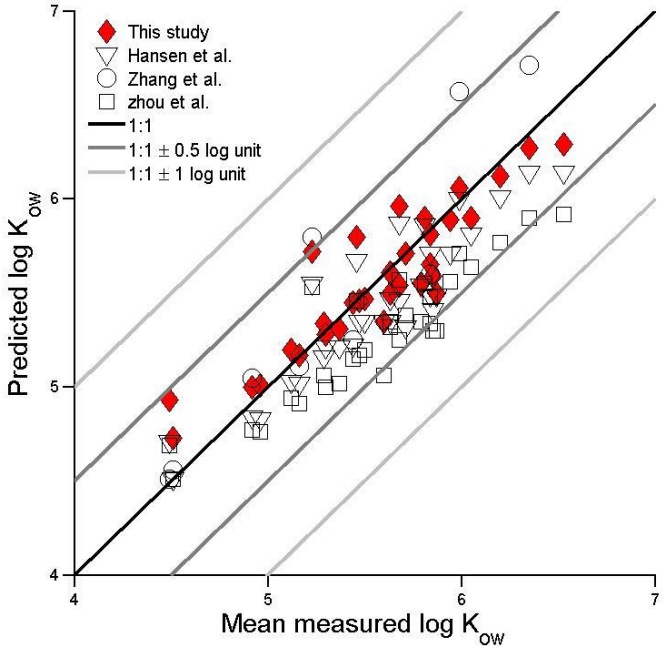

Figure 2.3 Predicted log K_{OW} from calculated polarizability (red diamonds), and commonly cited (open triangles and squares) or recent (open circles) poly-parameter predictive methods compared to measured log K_{OW} for polychlorinated biphenyls. The 1:1 line (black), 1:1 line ± 0.5 log unit (dark grey) and 1:1 line ± 1 log unit (light grey) are illustrated.

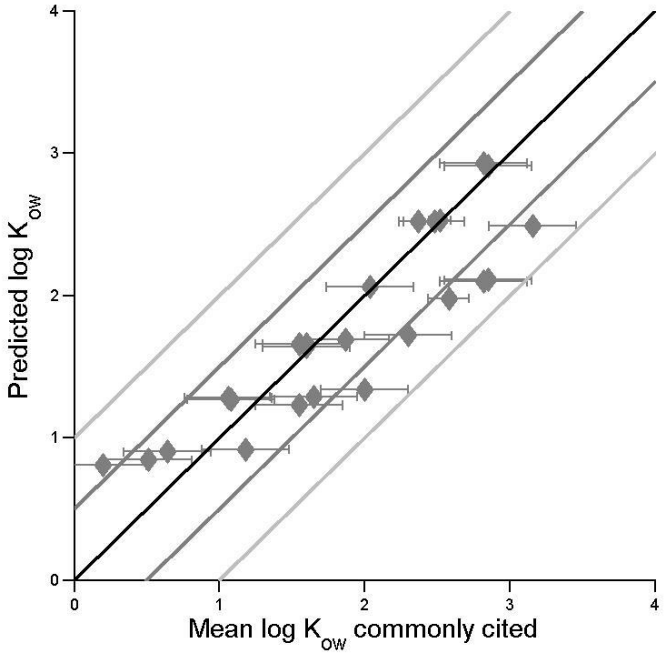

Figure 2.4 Predicted log K_{OW} from calculated polarizability and commonly cited predictive methods for fluorinated compounds. The 1:1 line (black); 1:1 line ± 0.5 log unit (dark grey) and 1:1 line ± 1 log unit (light grey) are illustrated.

This model is unique in that by applying basic thermodynamic arguments, it uses molecular polarizability as a single broadly applicable parameter for the prediction of K_{OW}. Thus, we show that a single-parameter SAR *can* successfully predict partitioning for a number of classes of compounds over a large K_{OW} range. The only commonality between the compound classes considered here is that inter-molecular interactions are dominated by dispersion forces. The model is able to predict the properties of alkanes, substituted benzenes, polyaromatics, biphenyls and brominated compounds. Furthermore, the validation set spans more than four orders of magnitude, from *log* $K_{OW} < 2$ to *log* $K_{OW} > 6.5$. This demonstrates the versatility of the method in predicting K_{OW} for compounds with a wide range of propensities to partition into octanol. The efficacy of the single-parameter as a predictor is demonstrated in Fig. 2.3, where predicted *log* K_{OW} values from the current SAR are compared to those from highly cited (Zhou et al. 2005; Hansen et al., 1999) and recent (Zhang et al., 2013) poly-parameter methods for PCBs.

Comparable predictive power is obtained from the single parameter of calculated polarizability compared to the multi-parameter models. In addition, each of the three multi-parameter models to which the polarizability model is compared was derived using solely PCBs for training and validation. It has been asserted that single-parameter SARs are typically useful only for compounds with very similar structures (Schwarzenbash et al., 2003). In the present model, a single parameter predicts *log* K_{OW} for diverse species with similar accuracy as poly-parameter models developed for a single class of compounds. We note that this model is not expected to be valid for compounds with intermolecular interactions other than dispersion forces.

Based on the thermodynamic basis described above, polarizability could be used as a descriptor and predictor for other condensed phase partitioning processes, which provides the possibility of polarizability as an indicator of more complexed processes, such as bioaccumulation in SML as well as in biota. BCF measurements are difficult to compare, because reported partitioning properties depend on numerous factors (e.g. species (Sagiura et al., 1979), exposure concentration (Oliver & Niini, 1983), temperature (Arnot & Frank, 2006), water quality (Arnot & Frank, 2006), etc.) that are not consistent between experiments. This leads to even greater variability in measurements than is observed between measurements of K_{OW}. Variability in measured BCFs for a single species can exceed four orders of magnitude (Mackay et al., 2004). Because of this, extensive work has focused on methods to relate K_{OW} to BCF (e.g. Neely et al. (1978), Maclay (1982)). The accurate prediction of K_{OW} and its use to determine BCF may be a more effective method to determine these parameters. Thus, the predictive method for K_{OW} using polarizability described here could be extended to inform BCF estimations.

Chapter 3. **Molecular polarizability as a single parameter to predict Bioconcentration factor**

3.1. Introduction

As an important ecological indicator, bioaccumulation potential in terms of bioconcentration factor is widely studied for the purpose of ecotoxicology evaluation of a chemical. The REACH requires BCF assessment for substance with manufactured or imported amount above 100 tonnes/year) (EURO, 2004). Ideally, the experimentally determined BCF data from field or laboratory-based food web model would be the most reliable; however, due to the complexity and the considerable cost of BCF tests, many researchers have looked for other methods to estimate BCF. Among them, using K_{OW} as a predictor is possible because octanol can be seen as a surrogate of natural organic matter including those found in organisms, so the uptake from water to octanol could be directly proportional to uptake from water to organisms (Schwarzenbach et al., 2004). BCF, which corresponds to the partitioning coefficient into biota from the environment (excluding food) has been shown to be correlated to the octanol−water partition coefficient. Correlations with K_{OW} are usually used as a preliminary screening tool for BCF when evaluating the property of a new chemical. Encouraged by the good correlation between polarizability and K_{OW}, we consider that the BCF, as partitioning coefficients between condensed phases, could also be described using polarizability. Under this assumption, we developed a novel model to predict BCF using polarizability as a single descriptor.

3.2. Methods

3.2.1. For microorganism BCF

Considering the much simpler structure and the metabolism of organic compounds in microorganism than other bioorganisms, we first studied the correlation between *log* BCF in microorganism (species unspecified) and polarizability with data for 27 chemical species (listed in Fig. S4) available in Mabey et al. (1982) to obtain a basic knowledge of the relationship.

3.2.2. For fish BCF

Fish are the most widely used target organism in BCF studies due to their position in the food chain and developed feeding techniques under controlled lab conditions, and hence there are matured operation protocols. Therefore, we used 82 *log* BCF data extracted from Japanese Ministry of International Trade and Industry (MITI) database (Japan Chemical Industry Ecology and Toxicology Information Center, Chemicals Inspection & Testing Institute, 1992) and regenerated by Dimitrov et al. (2005). The principles of data chosen in the experiment are 1) POPs containing F, Cl and/or Br; 2) *log* BCF data from the same fish species *Cyprinos carpio* with reported lipid content; 3) the experimental BCF data meets OECD 305 protocol criteria; 4) BCF data does not include the total amount of parent and metabolites chemistry but from the parent compounds only. Although previous studies showed that combining data from different species is acceptable when relating K_{OW} to BCF (Meylan et al., 1999), and that model based on different species yield similar results (Devillers, et al., 1996), this study did not include results from species other than *Cyprinos carpio* to reduce the uncertainties.

As discussed in Chapter 2, approximately three-quarters of data (62) were randomly chosen as the training set, leaving one-quarter (20) as the validation set.

The principles of selecting training and validation set and methods used to calculate polarizability are consistent with Chapter 2. A full list of compounds and their calculated polarizability values listed in Table S.3.

3.3. Results and Discussions

As unicellular organisms, microorganisms are the simplest creatures and fewer variables affect the uptake when partitioning into cell from water is concerned. For 27 compounds which have available microorganism *log* BCF data, Fig. 3.1 shows a very good linear correlation (r^2=0.89) between polarizability and BCF; therefore, polarizability could be a potential indicator of BCF for the microorganism.

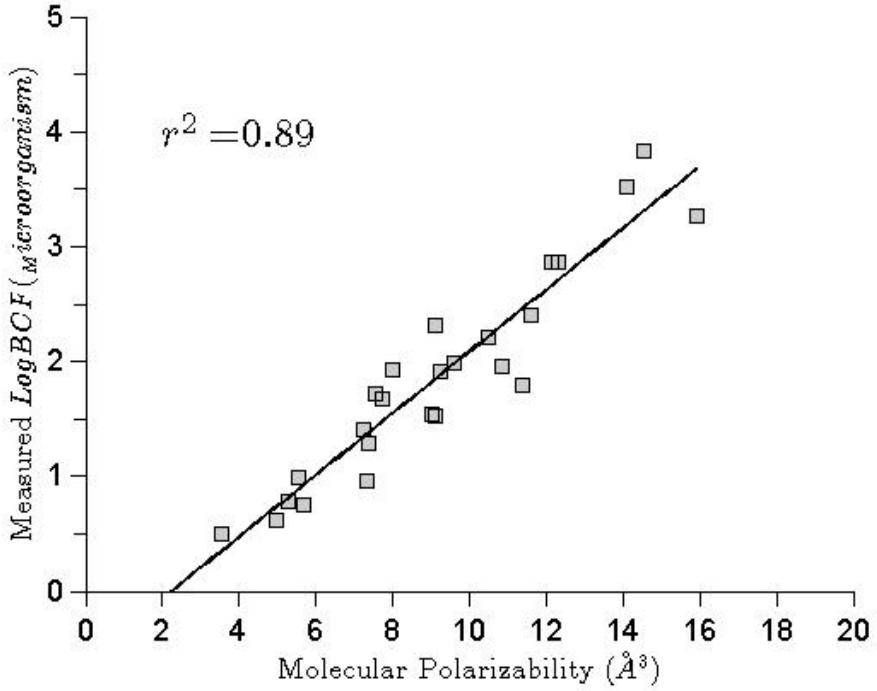

Figure 3.1 Correlation between molecular polarizability and measured log BCF in microorganism (species unspecified).

The results shown in Fig. 3.2 display a good linear correlation ($r^2 = 0.84$) between measured *log* BCF values and calculated polarizability for all 65 chlorinated, fluorinated, and brominated POPs chosen.

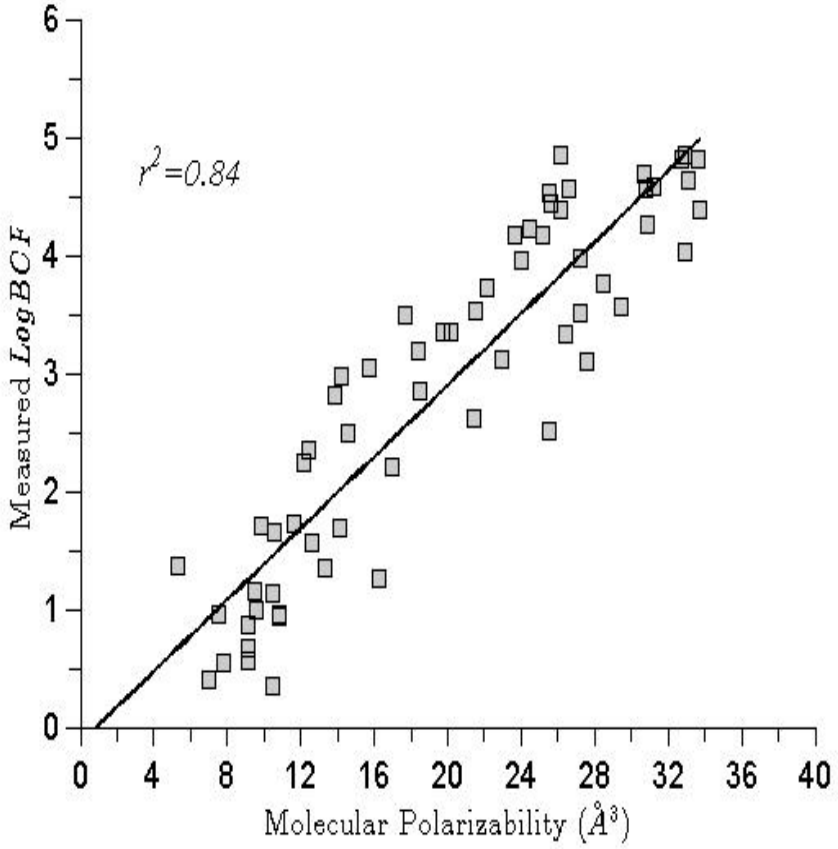

Figure 3.2 Correlation between median measured log BCF (Cyprinus carpio) and calculated molecular polarizability.

The predictive relationship derived using the regression:

$$\textit{log}\ \text{BCF} = (0.1516 \pm 0.0169)\ \alpha - (0.1414 \pm 0.0879) \qquad (3.1)$$

predicted the BCF of 77 out of 82 (89.0%) compounds within 1 *log* unit difference of measured BCF and 48 (58.5%) within 0.5 *log* unit (Fig. 3.3). This relationship can easily be applied to compounds with no BCF measurements. It can also distinguish the difference of structural isomers. Predicted *log* BCF values for all 286 compounds can be found in Table S.1.

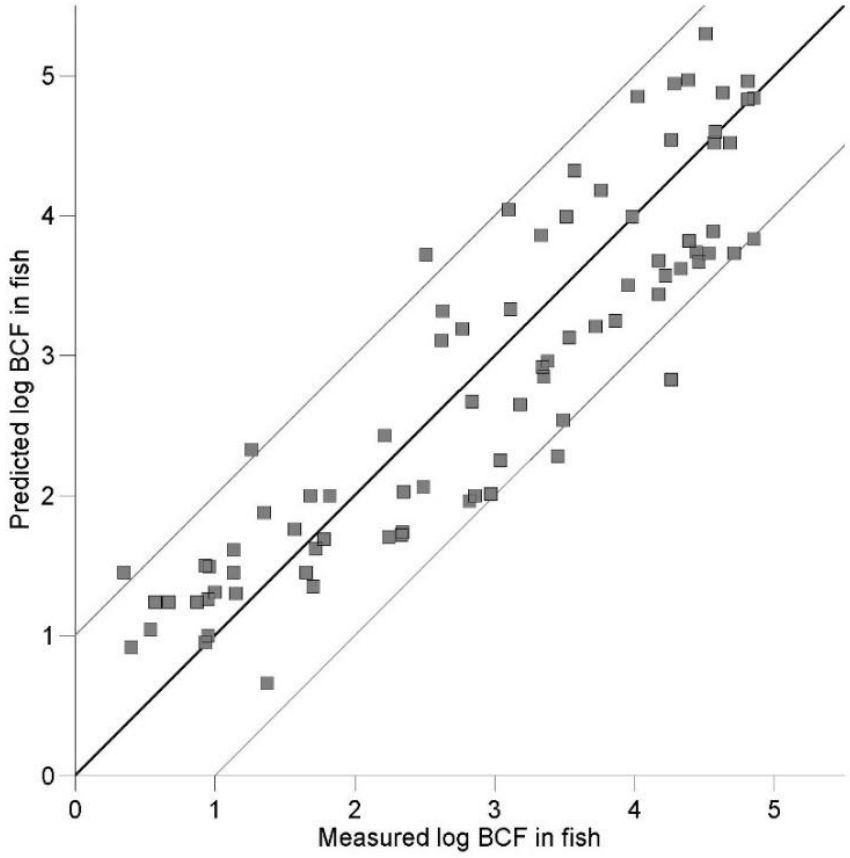

Figure 3.3 Predicted log BCF from calculated polarizability compared to measured log BCF

Previous studies showed that the correlation l*og* BCF/*log* K_{OW} tended to be linear for chemicals which had *log* K_{OW} ranging between 1 and 6 that were not metabolised. The linear trend began to break down when highly hydrophobic chemicals with *log* K_{OW}>6 were concerned. Given that the *log* K_{OW} of most target compounds in this study are lower than 6, a linear correlation is anticipated. Thus, the predictive method using polarizability as a single parameter can be extended to BCF estimations. Compared to previous published *log* K_{OW}/*log* BCF linear correlation results (e.g. Veith et al. (1979); Southworth et al. (1980); Mackay et al. (1982); Isnard & Lambert (1988); Geyer et al. (1991); and Dimitrov (2005)) , with r^2 ranged from 0.748 to 0.945, the presented method with r^2= 0.84 yield similar results to previous methods. The K_{OW}-

BCF model ignores the metabolic degradation of substances within a living organism and therefore tends to overestimate BCF (Pavan et al., 2006); the relationship described here does not suggest any overestimation, this may be contributed by the data selection. However, as a descriptor which can be directly calculated without any experimental data input, polarizability could be as a screening tool to indicate bioaccumulation potential when reliable experimental BCF data is not available.

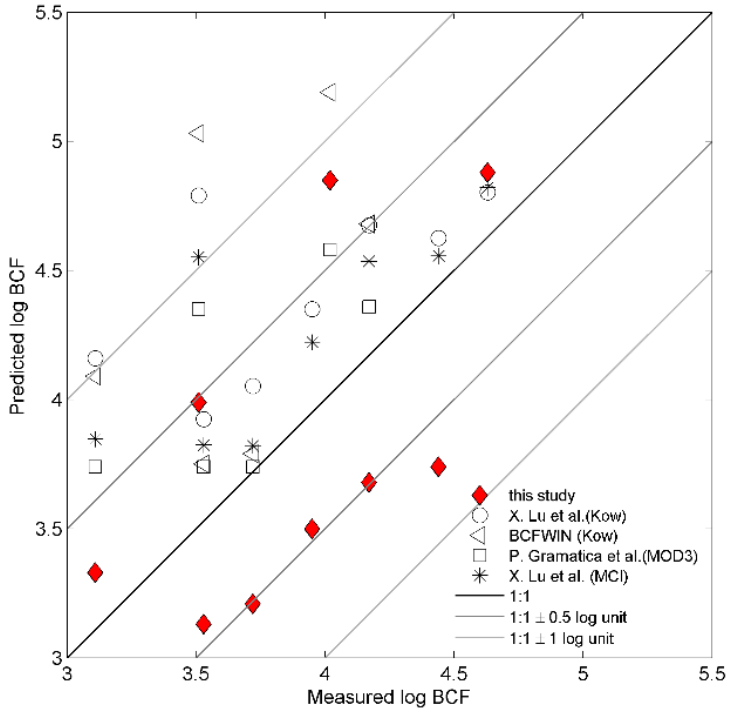

Figure 3.4 Predicted log BCF from calculated polarizability (red diamonds), and from recent (circle, triangle: based on KOW, square: 3D molecular, asteroid： MCI) poly-parameter predictive methods, denoted by their y locations, compared to measured log KOW, denoted by their x location, for polychlorinated biphenyls. The 1:1 line (black); 1:1±0.5 line (dark grey)； 1:1±1 line (light grey) are illustrated.

Fig. 3.4 shows a comparison among the *log* BCF of PCBs results obtained from different models based on KOW, 3D molecular descriptors or MCI (Lu et al., (2000); Gramatica & Papa (2003)). Most data are within 1 *log* unit difference, although BCF data sources are from different measurements (different fish species, equilibrium/kinetic methods, lipid content and weight of

the fish and exposure concentration and duration). It is notable that while data from other results tend to overestimate the BCF of PCBs, predictions from this study show a tendency to underestimate the BCF. This may reflect biotransformation as well as the potential error associated with the very high hydrophobicity of PCBs with measured *log* K_{OW} >5. In future work, we can enlarge the database to other species, such as rainbow trout, guppies, fathead minnows, bluegill sunfish, golden ide, etc.

Based the discussion above, BCF could now be estimated by polarizability, a fundamental parameter which can be directly calculated without recourse to K_{OW}. This method could be useful in ecotoxicology evaluation when no reliable data is available.

Chapter 4. **An improved glass plate SML sampling method using an auto squeegee**

4.1. Introduction

POPs, such as PBDEs, tend to concentrate into SML due to their hydrophobic properties. Polybrominated diphenyl ethers (PBDEs) were widely used as flame retardants, but many are now banned because of their environmental and health risks. Some PBDE congeners were designated as new POPs at the Stockholm Convention in 2009 (WHO, 2009). The process of bulk water-SML partitioning is vital when studying the fate of POPs such as PBDEs. As we already discussed, polarizability can be used as a single parameter to describe *log* K_{OW} and *log* BCF of a compounds. The SML, which is a layer of 'biofilm' could potentially also be described using polarizability. Although understanding of this partitioning is important to the fate and transport of POPs, there are only a few SML-water or SML-air partition coefficient studies up to the present (e.g. Monodori et al., 2006; Li et al., 2007). An improved understanding of POPs concentration is sub-surface water and surface microlayer is necessary to study the partition property concerning SML. However, SML sampling is always a time and energy consuming task. An efficient method is highly desirable, especially as the trace concentrations of POPs necessitate a relatively large sample volume. Based on the advantages and disadvantages discussed in Chapter 1, we improved the glass plate method with a commercially available auto squeegee and have tested this method by analyzing PBDEs in SML from a small local pond.

4.2. Materials and Method

4.1.1 Materials

All chemicals used in the experiments, except where noted, were purchased from OmniSolv™. The chemicals are HPLC grade. All the PBDEs standards (listed in Table 4.1) were purchased from Wellington Laboratories A dilution standard solution was prepared in acetone and stocked in -18 °C.

A customized glass plated of dimensions 30 cm*60 cm*4 mm was designed with two polypropylene handles fixed on (Fig.4.1(a)). When dipped in water and then lifted at a slow speed (approximately 3 cm/s), the plate can entrain SML water in top 100 μm (Harvey & Burzell, 1972).

A Karcher WV50 Power Squeegee Window Vacuum (Fig. 4.1(b)) was used instead of a traditional wiper to remove the sampled water off the glass plate into bottles. The squeegee is made of plastic polyvinyl chloride, polyethylene, and polypropylene. It grabs the water on glass surface into the built-in water tank. Detailed information of this equipment can be found at Karcher website (2016).

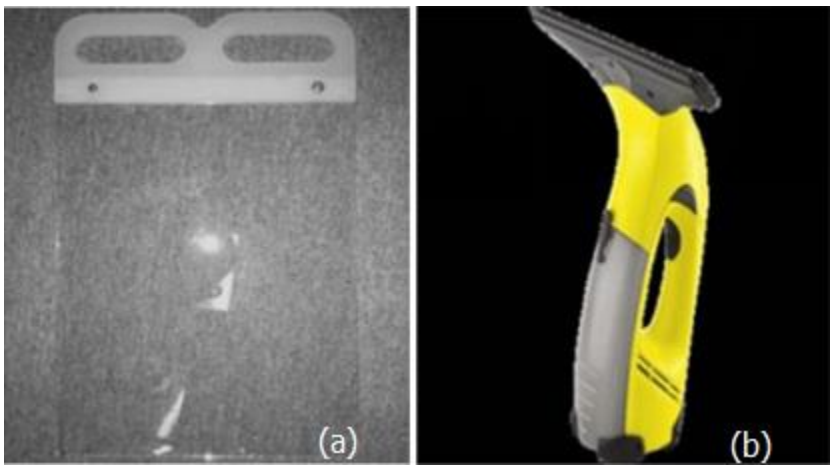

Figure 4.1 Pictures of glass plate (a) and auto squeegee (b).

2L polypropylene bottles and 100 mL polypropylene bottles were used as containers of the sampled water.

4.1.2 Sample Collection and Preparation

SML samples were collected in Long Pond, St. John's (47.5783° N, 52.7320° W). Long Pond is surrounded on one side by a large urban park, while the other side is a busy urban environment. Therefore, the pond is influenced by both natural process and human activities. SML samples were collected with a glass plate with a lift speed at about 3 cm/s, and subsurface water was collected at the same spot using bottles opened below water surface at 30 cm depth. Nano filtered water was used as field blank. The collected samples were labelled, filtered with a stainless steel pump under vacuum conditions using glass-fibre filters to remove particles and the obtained SML samples were stored at 4°C for further analysis. Analysis was done within 2 days after the sampling date to ensure the sample integrity.

4.1.3 Solid Phase Extraction (SPE) Methodology

A SPE isolation step was performed using a Supelco Visiprep 24 Vacuum Manifold filtration. An Oasis HLB SPE cartridge (3 cm^3, 100 mg) was preconditioned with 3 mL ethyl acetate followed by 3 mL nano filtered water. 100 mL DSML or 300 mL SSW sample was then loaded. A vacuum pump was used to aid the process. The speed was 1 drop s^{-1} and the vacuum was controlled within 20 mmHg.

3 mL methanol solution (40% v/v) was used in the cleaning stage to remove water and polar constituents. The cartridge was then air dried and eluted with 3 mL ethyl acetate and followed by 2 mL acetone. The solutions were combined, then dried under a stream of dry nitrogen and finally reconstituted in 0.5 mL acetone for GC-MS injection.

4.1.4 Gas Chromatography-Mass Spectrometry detection

Separation of PBDEs was performed using a DB 35 column (a (35%-phenyl)-methylpolysiloxane film, 0.25 mm i.d., 30 m long, with a film thickness of 0.25 μm) on an Agilent 7890 GC with He as a carrier gas. Analytes were detected by an Agilent 5875 MS using electron capture negative ionization with methane as the ionization gas. Injection volume was 1 μL at a temperature of 260ºC. The detection was in negative mode using SIM (Selected Ion Monitoring) acquisition method. A SIM *m/z* used to identify different PBDE congeners are listed in Table 4.1. The temperature program for the GC was as follows: an initial temperature of 70 ºC for 2 min, then rapidly increased at a rate of 20 ºC/min to 230 ºC and then increased to a final temperature of 270 ºC at a rate of 10 ºC /min and then was held at 270 ºC for 5min. The total run time was 24 min. Acetone was used as analytical blank. External standard was used as quantification method. Quantification was conducted with the abundance of *m/z* 79 only if the sample data were at least triple the blank value (S/N>3).

4.3. Results and Discussions

In theory, the SML thickness obtained by the glass plate method would be determined by sampling times of unit volume samples (n) and the area of the glass plate (A); however, in practice, a loss of collected sample can occur when being wiped down into the bottles. The auto squeegee used in this study is more efficient than a traditional wiper with a built-in water tank that minimized the loss of sample. It can collect 1 L SML sample from the surface of the glass plate in an hour with single-hand operation. Compared to traditional squeegee, which was reported to take up to 8 h to collect 1 L SML sample, this greatly reduced the time and effort required to collect a sample of SML. Furthermore, collection in a shorter time minimizes sample issues caused by spatial-temporal variability related to formation and persistence of SML

(Peltzer et al., 1992). The built-in water tank also greatly decreased the possibility of sample contamination from the air. The auto squeegee is affordable and economical considering the saved time and energy by the operator.

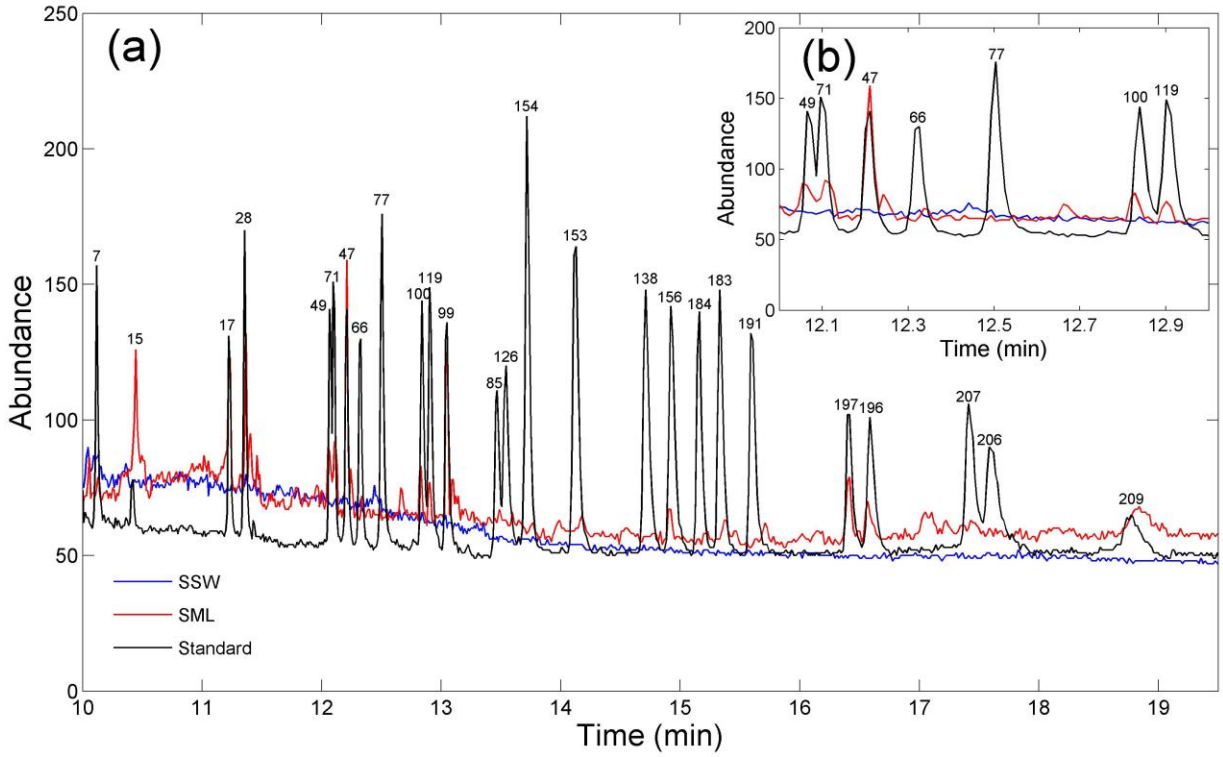

Figure 4.1 GC/MS Chromatogram of SSW, SML, and PBDE Standard. The labeled peaks are listed in Table 4.1

The GC-MS chromatogram of bulk water, SML and the standard are shown in Fig. 4.2. The result showed that PBDE 7 was detected only in subsurface water, while PBDE 15, 17, 28, 47, 49, 99, 100, 156, 196, 197, and 209 were detected in SML with 47 and 209 most abundant. BDEs-47, 99, 100, 183 and 209) are the main constituent of commercially available brominated products, so they are intensively detected in soil (Hassanin et al., 2004), water and sediment (Moon et al., 2012), and airborne particles (Deng et al., 2007). They are liable to photodegradation (Hagberg et al. 2006), microdegradation, and chemical degradation. This may

be attributed to the relative water-solubility of PBDE 7 compared to other congeners, which are much more hydrophobic. BDEs-47, 99, and 100 may come directly from PentaBDE and BDE-209 from DecaBDE, both of which were commonly used commercial mixtures. At the same time, BDE-209 can be photochemically and microbially degraded to BDEs-196, 197, 203, 99, and 100, (Tokarz et al., 2008; Lagalante et al., 2011) and gradually to 47 and 49, (Robrock et al. 2008). Further photodegradation and biodegradation can then lead to BDEs-15,17, and 28 (Wang et al., 2013). BDE-156 has been hardly reported in literature; the source of this compound is unknown. These results indicate that a larger sampling volume is required in order to obtain PBDE concentrations in water that are below the detection limit. Internal standard and extra preparation techniques can be used to decrease matrix effects. PBDEs in particulate SML were not studied in this preliminary experiment. A comparison between the traditional squeegee and the auto squeegee was not accomplished due to lack of time and changed environmental conditions (temperature, wind, etc.). Considering the materials used are similar, minimal differences in the quality of results is expected.

In future work, more data both from field work and lab conditions will be collected. With actual data, we can calculate the SML-water partition coefficient by:

$$K_{SWL-W} = \frac{C_{SML}}{C_{SSW}} = \frac{C_{DSML}+C_{PSML}}{C_{DSSW}+C_{PSSW}},$$

Where C_{SML} and C_{SSW} stand for the concentration of a compounds in SML and SSW respectively, C_{DSML} and C_{PSML} stands for the concentration of a compounds in DSML and PSML, C_{DSSW} and C_{PSSW} stands for the concentration of a compounds in DSSW and PSSW. And hence we can correlate the experiment data with calculated polarizability.

Table 4.1 Ion monitoring in PBDEs experiments and results

Congener No.	BDE	Ions monitored (*m/z*)	Window (min)	SSW (ng/L)	SML (ng/L)
7	2,4-Dibromodiphenyl ether	79.0,162.8,408.5,486.5	9.0-10.5	<LOQ	ND
15	4,4'-Dibromodiphenyl ether	79.0,162.8,408.5,486.5	9.0-10.5	ND	19.0
17	2,2'4-Tribromodiphenyl ether	79.0,162.8,408.5,486.5	9.0-10.5	ND	30.5
28	2,4,4'-Tribromodiphenyl ether	79.0,162.8,408.5,486.5	9.0-10.5	ND	25.0
47	2,2'4,4'-Tetrabromodiphenyl ether	79.0,162.8,403.0	10.0-12.5	ND	56.5
49	2,2',4,5'-Tetrabromodiphenyl ether	79.0,162.8,403.0	10.0-12.5	ND	<LOQ
66	2,3',4',6-Tetrabromodiphenyl ether	79.0,162.8,403.0	10.0-12.5	ND	ND
71	2,3',4,6-Tetrabromodiphenyl ether	79.0,162.8,403.0	10.0-12.5	ND	ND
77	3,3',4,4'-Tetrabromodiphenyl ether	79.0,162.8,403,483.0	10.0-12.5	ND	ND
85	2,2',3,4,4'-Pentabromodiphenyl ether	79.0,162.8,408.6,485.0,562.0	13.2-20.0	ND	ND
99	2,2',4,4',5-Pentabromodiphenyl ether	79.0,162.8,483.0	12.5-13.2	ND	<LOQ
100	2,2',4,4',6-Pentabromodiphenyl ether	79.0,162.8,483.0	12.5-13.2	ND	<LOQ
119	2,3',4,4',6-Pentabromodiphenyl ether	79.0,162.8,483.0	12.5-13.2	ND	ND
126	3,3',4,4',5-Pentabromodiphenyl ether	79.0,162.8,406.6,485.0,562.0	13.2-20.0	ND	ND
138	2,2',3,,4,4',5'-Hexabromodiphenyl ether	79.0,162.8,408.6,485.0,562.0	13.2-20.0	ND	ND
153	2,2',4,4',5,5'-Hexabromodiphenyl ether	79.0,162.8,408.6,485.0,562.0	13.2-20.0	ND	ND
154	2,2',4,4',5,6'-Hexabromodiphenyl ether	79.0,162.8,408.6,485.0,562.0	13.2-20.0	ND	ND
156	2,3,3',4,4',5-Hexabromodiphenyl ether	79.0,162.8,408.6,485.0,562.0	13.2-20.0	ND	<LOQ
183	2,2',3,4,4',5',6-Heptabromodiphenyl ether	79.0,162.8,408.6,485.0,562.0	13.2-20.0	ND	ND
184	2,2',3,4,4',6,6'-Heptabromodiphenyl ether	79.0,162.8,408.6,485.0,562.0	13.2-20.0	ND	ND
191	2,3,3'4,4',5',6-Heptabromodiphenyl ether	79.0,162.8,408.6,485.0,562.0	13.2-20.0	ND	ND
196	2,2'3,3',4,4',5,6'-Octabromodiphenyl ether	79.0,162.8,408.6,485.0,562.0	13.2-20.0	ND	15.3
197	2,2'3,3',4,4',6,6'-Octabromodiphenyl ether	79.0,162.8,408.6,485.0,562.0	13.2-20.0	ND	24.0
206	2,2'3,3'4,4',5,5',6-Nonabromodiphenyl ether	79.0,162.8,408.6,485.0,562.0	13.2-20.0	ND	ND
207	2,2'3,3'4,4',5,6,6'-Nonabromodiphenyl ether	79.0,162.8,408.6,485.0,562.0	13.2-20.0	ND	ND
209	Decabromodiphenyl ether	79.0,162.8,408.6,485.0,562.0	13.2-20.0	ND	37.5

ND means 'not detected', <LOD

<LOQ means that S/N is between 3~10.

Chapter 5. **Conclusions and Future Work**

This thesis discussed the ability of polarizability as a single parameter to predict *log* K_{OW} and *log* BCF (in microorganism and fish). Least Square Fit was employed in this study to build a linear correlation between the two parameters with three-quarters of the total data used as a training set and one-quarter used as a validation set.

The results showed that both *log* K_{OW} (Chapter 2) and *log* BCF (Chapter 3) can be calculated with molecular polarizability with a good prediction power. For *log* K_{OW}, the prediction power can reach 0.92 and 0.84 for *log* BCF in fish. Compared to poly-parameter models, this method employs only the input of polarizability, which can be easily calculated by computational software. The merit of this model is that it carries physical-chemistry meaning; besides, it can distinguish different chemical isomers. Molecular polarizability can be an easy indicator of the possible environmental fate, bioaccumulation properties of a new compound. The data used in the proposed BCF calculating model is from a single fish species (*Cyprinos Carpio*). In future work, more data from other sources for different fish species could be included in the model to enlarge the application scope.

With limited BCF microorganism data, the correlation between polarizability and *log* BCF is also significant with r^2=0.89, which suggests that molecular polarizability could be a good predictor for the partition concerning SML as well. A basic SML-water partition model is described by Fig 5.1. As mentioned in Chapter 1, SML is a physicochemically complex gelatinous film, therefore, the partition properties between SML and water would be analogous to that of the BCF between microorganism and water, both of which represent the partition property into a monomolecular layer from water phase. In future work, we will gather enough

POPs concentration in SML and SSW information to get a basic knowledge of POPs in SML and then will correlate polarizability with $K_{SML\text{-}W}$.

The proposed glass plate sampling method can be customized and improved in future work. Under the same conception, we can build a device which can simultaneously wipe both sides of a glass plate therefore achieve even greater sampling efficiency.

References

U.S. Environmental Protection Agency. (2012). Retrieved from Terminology Services (TS): http://ofmpub.epa.gov/sor_internet/registry/termreg/searchandretrieve/glossariesandkeywordlists/search.do?details=&glossaryName=Eco%20Risk%20Assessment%20Glossary

Abd-Allah, A.M.A. (1999). Organochlorine contaminants in microlayer and subsurface water of Alexandria Coast. Egypt. *Journal of AOAC International*, 82, 391–398.

ACD. (2001). ACD logP. Toronto,ON: *Adcanced Chemistry Development*.

Arnot, J. A., & Gobas, F. A. (2004). A food web bioaccumulation model for organic chemicals in aquatic ecosystems. *Environmental Toxicology & Chemistry*, 23(10), 2343–2355.

Arnot, J., & A.P.C., F. (2006). A review of bioconcentration factor (BCF) and bioaccumulation factor (BAF) assessments for organic chemicals in aquatic organisms. *Environmental Reviews*, 14(4), 257-297.

Arnot, J., & Gobas, F. (2006). A process by which there is a net accumulation of a chemical directly from an exposure medium into an organism. *Environmental Reviews*, 14, 257-297.

Audry, E., Dubost, J. P., Collecter, J. C., & Dallet, P. (1986). A novel approach of structure-activity relationship: molecular lipohipicity potential . *Journal of Medicinal Chemistry*, 21, 1-72.

Babujee, J. B. (2012). Topological Indices and New Graph Structures. *Applied Mathematical Sciences*, 108(6), 5383-5401.

Bintein, S., Devillers, J., & Karcher, W. (1993). Nonlinear dependenceof fish bioconcentration onn-octanol/water partition coefficient. *SAR QSAR Environment Research*, 1, 29-39.

Bodor, N., & Buchwald, P. (1997). Molecular Size Based Approach To Estimate Partition Properties for Organic Solutes. *Journal of Physical Chemistry B*, 101(17), 3404–3412.

Bodor, N., & Huang, M. (1992). An extended version of a novel method for the estimation of partition coefficients. *Journal of Pharmacy Science*, 81(3), 272-281.

Bodor, N., Gabany, Z., & Wong, C. (1989). A new method for the estimation of partition coefficient. *Journal of the American Chemical Society*, 11, 3783-3786.

Bowman, B., & Sans, W. (1983). Determination of octanol-water partitioning coefficient (Kow) of 61 organophosphorous and carbamate insecticides and their relationship to respective water solubility (S) values. *Journal of Enviromental Science & Health*, B18(6), 667-683.

Chiou, C., Schmedding, D. W. & Manes, M. (2005). Improved prediction of octanol-water partition coefficients from liquid-solute water solubilities and molar volumes. *Environmental Science and Technology*, 39, 8840-8846.

Compudrug Ltd. (1992). PrologP. Budapest.

Connell, D. W. & Hawker, D. (1988). Use of polynomial expressions to describe the bioconcentration of hydrophobic chemicals by fish. *Ecotoxicology and Environmental Safety*, 16, 242-257.

Connell, D. W., Wu, R. S., Richardson, B. J., Leung, K., Lam, P. S., & Connell, P. A. (1998). Fate and risk evaluation of persistent organic contaminants and related compounds in Victoria Harbour, Hong Kong. *Chemosphere*, 36, 2019-2030.

Cunliffe, M. U.G. (2011). Microbiology of aquatic surface microlayers. *FEMS Microbiol Rev*, 35, 233-246.

Macek, K. J., Petrocelli, S. R., & Carroll, J. (1980). An evaluation of using partition coefficients and water solubility to estimate bioconcentration factors for organic chemicals in fish. *American Society for Testing and Materials* (pp. Eaton JG, Parrish PR, Hendricks AC, eds, Aquatic Toxicology,STP 707). Philadelphia, PA: 116-129.

Deng, W. J., Zheng, J. S., Bi, X. H., Fu, J. M., & Wong, M. H. (2007). Distribution of PBDEs in air particles from an electronic waste recycling site compared with Guangzhou and Hong Kong, South China. *Environment International*, 33(8), 1063-1069.

Devillers, J., Domine, D., Guillon, C., & Karcher, W. (1998). Simulating lipophilicity of organic molecules with a back-propagation neural network. *Journal of Pharmaceutical Sciences*, 87(5), 1086–1090.

Devillers, J., Bintein, S., & Domine, D. (1996). Comparison of BCF models based on log P. *Chemosphere*, 33(6), 1047-1065.

Dimitrov S., D. N. (2005). Base-line model for identifying the bioaccumulation potential of chemicals. *SAR QSAR Enviromental Research*, 16, 531-554.

Duce, R.A., Quinn, J.G., Olney, C.E., Piotrowicz, S.R., Ray, B.J., Wade, T.L. (1972). Enrichment of heavy metals and organic compounds in the surface microlayer of Narragansett Bay, Rhode Island. *Science*, 176, 161–163.

Ema, M., Fujii, S., Hirata-Koizumi, M., & Matsumoto, M. (2008). Two-generation reproductive toxicity study of the flame retardant hexabromocyclododecane in rats. *Reproductive Toxicology*, 25(3), 335-351.

Falkowska, L. (1999). Sea surface microlayer: a field evaluation of teflon plate, glass plate and screen sampling techniques. Part 1. Thickness of microlayer samples and relation to wind speed. *Oceanologia*, 41(2), 211-221.

Frisch, M. J., Trucks, G. W., Schlegel, H. B., Scuseria, G. E., Robb, M. A., Cheeseman, J. R., et al. (1998). *Gaussian 98*, Revision A.7. Gaussian, Inc., Pittsburgh, PA.

Gaillard, P., Carrupt, p., Testa, B., & Boudon, A. (1994). Molecular Lipophilicity Potential, a tool in 3D QSAR: Method and applications. *Journal of Computer-Aided Molecular Design*, 8(2), 83-94.

Geyer, H. J., Scheunert, I., Briiggemann, r., Steinberg, C., Korte, F., & Kettrup, A. (1991). QSAR for organic chemical bioconcentration in Daphnia, algae, and mussels. *The Science of the Total Environment* 109/110, 387-394.

Gramatica, P., & Papa, E. (2003). QSAR modelling for bioconcentation factor by theoretical molecular descriptors. *QSAR & Combinatorial Science*, 22, 374-385.

Griffin, S. W. (1999). Determination of octanol–water partition coefficient for terpenoids using reversed-phase high-performance liquid chromatography. *Journal of Chromatography A*, 864(2), 221-228.

Haeberlein, M., & Brinck, T. (1997). Prediction of water–octanol partition coefficients using theoretical descriptors derived from the molecular surface area and the electrostatic potential. J*ournal of the Chemical Society, Perkin Transactions*, 2, 289-294.

Hagberg, J., Olsman, H., Van Bavel, B., Engwall, M., & Lindström, G. (2006). Chemical and toxicological characterisation of PBDFs from photolytic decomposition of decaBDE in toluene. *Environment international*, 32(7), 851-857.

Hamelink, J., Waybrant, R., & Ball, R. (1971). proposal: exchange equilibria control the degree chlorinated hydrocarbons are biologically magnified in lentic environment.

Hansch, C., & Leo, A. J. (1979). *Substituent Constants for Correlation Analysis in Chemistry and Biology*. New York: Wiley.

Hansen, B. G., Paya-Perez, A. B., Rahman, M., & Larsen, B. R. (1999). QSARs for Kow and Koc of PBD congeners: A critical examination of data, assumptions and statistical approaches. *Chemosphere*, 39, 2209-2228.

Harvey, G. (1966). Microlayer collection of sea surface: A new method and intial results. *Limnology and Oceanography*, 4, 608-613.

Harvey, G. (2003). Microlayer collection from the sea surface: A new method and intitial results. *Limnology and Oceanography*, 11(4), 608-613.

Harvey, G. W., & Burzell, L. (1972). Simple microlayer method for small samples. *Limnology and Oceanography*, 17, 156-157.

Harvey, G., & Burzell, L. (2003). A simple microlayer method for small samples . *Limnology and Oceanography*, 17(1), 156-157.

Hassanin, A., Breivik, K., Meijer, S. N., Steinnes, E., Thomas, G. O., & Jones, K. C. (2004). PBDEs in European background soils: levels and factors controlling their distribution. *Environmental science & technology*, 38(3), 738-745.

Hawker, D., & Connell, D. (1988). Influence of partition coefficient of lipophilic compounds on bioconcentration kinetics with fish. *Water Research*, 22(6), 701-707.

Hendrik Timmerman, H., Todeschini, R. T., Consonni, V., Mannhold, R., & Kubinyi, H. (2002). *Handbook of Molecular Descriptors*. Weinheim: Wiley-VCH.

Hickey, A. L., & Rowley, C. N. (2014). Benchmarking quantum chemical methods for the calculation of molecular dipole moments and polarizabilities. *Journal of Physical Chemistry A*, 118(20), 3678-3687.

Howard, P., Boethling, R., Jarvis, W., Meylan, W., & Michalenko, E. (1991). *In Handbook of Environmental Degradation Rates*.. Chelsea, MI: Printup, H.T. (ed), Lewis Publishers, 9.

Hu, J., Liang, Y., Chen, M., & Wang, X. (2009). Assessing the Toxicity of TBBPA and HBCD by Zebrafish Embryo Toxicity Assay and Biomarker Analysis. *Environmental Toxicology*, 8, 334-342.

Isnard, P., & Lambert, S. (1988). Estimating bioconcentration factors from octanol–water partition coefficient and aqueous solubility. *Chemosphere*, 17, 21-34.

Isrealachvili, J. (1992). *Intermolecular and Surface Forces*. 2nd ed. San Diego: Academic Press.

Leo, A., & Weininger, D. (1989). Medchem Software Manual. Irvine,CA: *Daylight Chemical Information Systems*.

Kärcher GmbH & Co, 2016. Product Manual for WV 50 *EU (Part number 1.633-100.0).Retrieved fromhttp://www.karcher.com/int/products/Home__Garden/Window_cleaner/16331000.htm.

Lagalante, A. F., Shedden, C. S., & Greenbacker, P. W. (2011). Levels of polybrominated diphenyl ethers (PBDEs) in dust from personal automobiles in conjunction with studies on the photochemical degradation of decabromodiphenyl ether (BDE-209). *Environment international*, 37(5), 899-906.

Letcher, R., Bustnes, J., Dietz, R., Jenssen, B., Jørgensen, E., Sonne, C., et al. (2010). Exposure and effects assessment of persistent organohalogen contaminants in Arctic. *Science of the Total Environment*, 410, 2995-3043.

Li, Y. F., Macdonald, R. W. (2005). Sources and pathways of selected organochlorine pesticides to the Arctic and the effect of pathway divergence on HCH trends in biota: a review. *Science of Total Environment*, *342*, 87-106.

Li, H., Ellis, D., Mackay, D. (2007). Measurement of Low Air−Water Partition Coefficients of Organic Acids by Evaporation from a Water Surface. *Journal of Chemical & Engineering Data, 52* (5), 1580-1584

Linkov, I., Ames, M. R., Crouch, E. A., & Satterstrom, F. K. (2009). Uncertainty in octanol-water partition coefficient: Implications for risk assessment and remedial costs. *Environment Science & Technology*, 39, 6917-6922.

Liss, P. D. (1997). *The Sea Surface and Global Change*. Cambridge: Cambridge University Press.

Lombardo, A., Roncaglioni, A., Boriani, E., Chiara Milan, C., & Benfenati, E. (2010x). Assessment and validation of the CAESAR predictive model for bioconcentration factor(BCF) in fish. *Chemistry Central Journal*: 4(S1).

Lu, X., Tao, S., Hu, H., & Dawsom, R. W. (2000). Estimation of bioconcentration factors of nonionic organic compounds in fish by molecular connectivity indices and polarity correction factors. *Chemosphere*, 41, pp. 1675-1688.

Mabey, W. S. (1982). In Aquatic Fate Process Data for Organic Priority Pollutants (EPA-44/4-81-014; NTS PB87-1690) (pp. 179-180). Washington, DC: Office of Water Regulations and Standards, US Environmental Protection Agency.

Machatha, S. G., & Yalkowsky, S. H. (2005). Comparison of the octanol/water partition coefficients calculated by ClogP, ACDlogP and KowWin to experimentally determined values . *International Journal of Pharmaceutics*, 294(1), 185-192.

Mackay, D. (1982). Correlation of bioconcentration factors. *Environmental Science & Technology*, 16, 274-278.

Mackay, D., Paterson, S., Kicsi, G., Di Guardo, A., & Cowan, C. E. (1996). Assessing the fate of new and existing chemicals: A five stage process. *Environmental Toxicology& Chemistry*, 15, 1618-1626.

Mackay, D., Shiu, W., Ma, K., & Lee, S. C. (2006). *Handbook of Physical-Chemical Properties and Environmental Fate for Organic Chemicals, Second Edition*. Boca Raton, FL: CRC Press.

Makino, M. (1998). Prediction of n-octanol/waterpartition coefficients of polychlorinated biphenyls by use of computer calculated molecular properties. *Chemosphere*, 37(1), 13-26.

Mannhold, R., & Petrauskas, A. (2003). Substructure and whole molecule approaches for calculating log P. *QSAR & Combinatorial Science*, 5, 466-475.

Mannholda, R., & van de Waterbeemd, H. (2001). Substructure and whole molecule approaches for calculating log P. *Journal of Computer-Aided Molecular Design*, 15, 337-354.

Manodori, L., Gambaro, A., Piazza, R., Ferrari, S., Stortini, A. M., Moret, I., & Capodaglio, G. (2006). PCBs and PAHs in sea-surface microlayer and sub-surface water samples of the Venice Lagoon (Italy). *Marine Pollution Bulletin*, 52(2), 184-192.

Meylan, W. (1993). *SRC-LOGKOW for Windows*. Syracuse, N.Y.: SRC.

Meylan, W., & Howard, P. (1995). Atom/fragment contribution method for estimating octanol-water partition coefficients. *Journal of pharmaceutical sciences*, 84, 83-92.

Meylan, W. M., Howard, P. H., Boethling, R. S., Aronson, D., Printup, H., & Gouchie, S. (1999). Improved method for estimating bioconcentration/bioaccumulation factor from octanol/water partition coefficient. *Environmental Toxicology and Chemistry*, 18(4), 664-672.

Moon, H. B., Choi, M., Yu, J., Jung, R. H., & Choi, H. G. (2012). Contamination and potential sources of polybrominated diphenyl ethers (PBDEs) in water and sediment from the artificial Lake Shihwa, Korea. *Chemosphere*, 88(7), 837-843.

Moriguchi, I., Hirono, S., Liu, Q., Nakagome, I., & Y., M. (1992). Simple method of calculating octanol/water partition coefficient. *Chemical and Pharmaceutical Bulletin*, 40, 127-130.

Neely, W. B., Branson, D. R., & Blau, G. E. (1978). Partition coefficient to measure bioconcentraion potential of organic chemicals in fish. *Environmental Science & Technology*, 8, 1113-1116.

New York State Department of Environmental Conservation. (n.d.). Division of Water Technical and Operational Guidance Series (1.1.4): Guidelines for deviatiion of bioacumulation factors. NY.

OECD. (1995). Test No. 107: Partition Coefficient (n-octanol/water): Shake Flask Method. In OECD Guidelines for the Testing of Chemicals, Section 1. Paris: OECD Publishing.

OECD. (1996). No.305E: Bioconcentration: Flow-through fish test. In OECD guidelines for the testing chemicals (p.23). Paris: OECD Publishing.

OECD. (2002). OECD Series on Testing and Assessment Harmonised Integrated Classification System for Human Health and Environmental Hazards of Chemical Substances and Mixtures. In OECD Guidelines for the Testing of Chemicals (p.193). Paris: OECD Publishing.

OECD. (2004). Partition Coefficient (octanol-water): High performance liquid chramotagraphy. In OECD guidline for the testing chemicals (p.1-11). Paris: OECD Publishing.

OECD. (2006). Test 123 Partition Coefficient (1-Octanol/Water): Slow-Stirring Method. In OECD guidelines for the testing chemicals (p.1-15). Paris: OECD Publishing.

Oliver, B. G., & Niini, A. J. (1983). Bioconcentration of chlorobenzenes from water by rainbow trout: correlations with partition coefficients and environmental residues. *Environmental Science & Technology*, 17, 287-291.

Pavan, M., Worth, A. P., & Netzeva, T. I. (2006). Review of QSAR Models for Bioconcentration. Ispra, Italy: European Commission, Joint Research Center.

Peltzer, R. D., Griffin, O. M., Barger, W. R., & Kaise, J. A. (1992). High-resolution measurements of surface-active film redistribution in ship wakes. *Journal of Geophysical Research*, 97, 5231–5252.

Petrauskas, A. A., & Kolovanov, E. A. (2000). ACD/Log P method description. *Perspectives in Drug Discovery and Design*, 19, 99-106.

Registration, E. A. (2006). CAESAR Bioconcentration Factor. Retrieved 01 12, 2016, from http://www.caesar-project.eu/index.php?page=results&section=endpoint&ne=1

Ritter, L., Solomon, K., Forget, J., Stemeroff, M., & O'Leary, C. (2007). Persistant Organic Pollutants:An Assessment Report on:DDT-Aldrin-Dieldrin-Endrin-Chlordane,Heptachlor-Hexachlorobenzene,Mirex-Toxaphene,Polychlorinated Biphenyls,Dioxins and Furans. Guelph, ON, Canada: United Nations Environment Programme.

Robrock, K. R., Korytár, P., & Alvarez-Cohen, L. (2008). Pathways for the anaerobic microbial debromination of polybrominated diphenyl ethers. *Environmental Science & Technology*, 42(8), 2845-2852.

Sagiura, K., Washino, T., Hattori, M., Sato, E., & Goto, M. (1979). Accumulation of organochlorines in fihses- dififference of accumulation factors by fishes. *Chemosphere*, 6, 359-364.

Sangster, J. (1997). *Octanol-water partition coefficients—fundamentals and physical chemistry*. New York: Wiley.

Sangster, M. (1989). Octanol-water partition coefficients of simple organic compounds. *Journal of Physical and Chemical Reference Data*, 18(3), 1111-1127.

Schwarzenbach, R. P., Gschwend, P. M., & Imboden, D. M. (2003). *Environmental Organic Chemisty*. Hoboken , New Jersey: John Wiley and Sons.

Schwarzenbach, R., Gschwend, P., & Imoden, D. (2004). *Environmental Organic Chemistry*. New Jersey: John Wiley & Sons.

Shinki, M., Wendeberg, M., Vagle, S., Cullen, J., & Hore, D. K. (2012). Characterization of absorbed microlayer thickness on an oceanic glass plate sampler. *Limnology and Oceanography*: *Methods*, 40, 728-735.

Sieburth, J. (1983). *Microbiological and organic-chemical processes in the surface and mixed layers. In S. W. Liss P.S., Air-Sea Exchange of Gases and Particles* (p.121-172). Hingham, MA: Reidel Publishers Company.

Sinkkonen, S., & Paasivirta, J. (2000). Degradation half-life times of PCDDs, PCDFs and PCBs for environmental fate modeling. *Chemosphere*, 40, 943-949.

Southworth, G. R., Keffer, C., & Beauchamp, J. J. (1980). Potential and realized bioconcentration. A comparison of observed and predicted bioconcentration of azaarenes in the fathead minnow (Pimephales promelas). *Environmental Science & Technology*, 14, 1529–1531.

Staikova, M., Messih, P., Lei, Y. D., Wania, F., & Donaldson, D. J. (2005). Prediction of subcooled vapor pressures of nonpolar organic compounds using a one-parameter QSPR. *Journal of Chemical and Engineering Data*, 50, 438-443.

Staikova, M., Wania, F., & Donaldson, D. J. (2004). Molecular polarizability as a single-parameter predictor of vapour pressures and octanol-air partitioning coefficients of non-polar compounds : a priori approach and results. *Atmospheric Environment*, 38, 213-225.

Stortini, A., Martellini, T., Del Bubba, M., Lepri, L., Capodaglio, G., & Cincinelli, A. (2009). n-Alkanes, PAHs and surfactants in the sea surface microlayer and sea water samples of the Gerlache Inlet sea (Antarctica). *Microchemical Journal*, 92, 37-43.

Tokarz Iii, J. A., Ahn, M. Y., Leng, J., Filley, T. R., & Nies, L. (2008). Reductive debromination of polybrominated diphenyl ethers in anaerobic sediment and a biomimetic system. *Environmental Science & Technology*, 42(4), 1157-1164.

Tolls, J., Bodo, K., DujardIn, K., Kim, Y., Moeller-Jensen, L., Mullee, D., et al. (2003). Slow-stirring method for determining the n-octanol/water partition coefficient (Pow) for highly hydrophobic chemicals: performance evaluation in a ring test. *Environmental Toxicology Chemistry*, 22(5), 1051-1057.

U. S. Envrironmeal Protection Agency. (2012). *Estimating Persistence, Bioaccumulation, and Toxicity Using the PBT Profiler*. In Sustainable Futures / P2 Framework Manual 2012 EPA-748-B12-001 (p. 7-3).

United States Environmental Protection Agency. (2012). *Estimation Programs Interface Suite™ for Microsoft® Windows*, v 4.11. Washington, DC, USA.

US Environment Protection Agency, E. F. (1989). *Pesticide Environmental Fate One Line Summary: DDT* (p, p'). Washington, DC.

Valkó. (2004). Application of high-performance liquid chromatography based measurements of lipophilicity to model biological distribution . *Journal of Chromatography A*, 299-310.

Vallack, H. W., Bakker, D. J., Brandt, I., Broström-Lundén, E., Brouwer, E., Bull, K. R., et al. (1998). Controlling persistent organic pollutants–what next? *Environmental Toxicology and Pharmacology*, 6, 143-175.

van der Ven, L. T. (2009). Endocrine effects of hexabromocyclododecane (HBCD) in a one-generation reproduction study in Wistar rats. *Toxicology letters*, 185(1), 51-62.

Van Pinxteren, M., Fombda, W., & Muller, K. H. (2012). *Determination of organic matter in oceanic water samples and the corresponding marine aerosol*. Retrieved from http://chemie.tropos.de/: http://chemie.tropos.de/Poster/MvP/poster-kiel-final-mvp.pdf

Veith, D. G., DeFoe, D. L., & Bergstedt, B. (1979). Measuring and estmating the bioconcentration factor of chemicals in fish. *Journal of the Fisheries Research Board of Canada*, 36, 1040–1048.

Walters, D. M., Mills, M. A., Cade, B. S., & Burkard, L. P. (2011). Trophic magnification of PCBs and its relationship to the octanol-water partition coefficient. *Environmental Science& Technology*, 45(9), 3917–3924.

Wang, X., Yao, T., Cong, Z., Yan, X., Kang, S., & Zhang, Y. (2006). Gradient distribution of persistent organic contaminants along northern slope of central-Himalayas, China. *Science of the Total Environment*: 372, 193-202.

Wang, J. Z., Hou, Y., Zhang, J., Zhu, J., & Feng, Y. L. (2013). Transformation of 2, 2′, 4, 4′-tetrabromodiphenyl ether under UV irradiation: Potential sources of the secondary pollutants. *Journal of hazardous materials*, 263, 778-783.

Wania, F., & Mackay, D. (1996). Tracking the Distribution of Persistent Organic Pollutants. *Environment Science & Technology*, 30(9), 390-396.

Wells, P. R. (1963). Linear free energy relationships. *Chemical Reviews*, 63(2), 171-219.

Williams, P.M., Robertson, K.J. (1973). Chlorinated hydrocarbons in sea-surface films and subsurface waters at nearshore stations and in the North Central Gyre. *Fishery Bulletin*, 73, 445–447

Wittekindt, C., & Goss, K.-U. (2009). Screening the partition behavior of a large number of chemicals with a quantum-chemical software. *Chemosphere*, 76, 460-464.

Wu, C., Wei, D., Liu, X., Lin, Z., & Wang, L. (2002). Evaluation of three models for predicting newly determined octanol-water partition coefficients and mechanisms for substituted aromatic compounds. *Water Environmental Research*, 74, 242-247.

Wurl, O., Obbard J.P. (2005) Chlorinated pesticides and PCBs in the sea-surface microlayer and seawater samples of Singapore, *Marine Pollution Bulletin*, 50, 1233–1243

Yu, S., Gao, S., Gan, Y., Zhang, Y., Ruan, X., Wang, Y., ... & Shi, J. (2016). QSAR models for predicting octanol/water and organic carbon/water partition coefficients of polychlorinated biphenyls. *SAR and QSAR in Environmental Research*, 27(4), 249-263.

Young, C. F. (2007). Perfluorinated acids in Arctic snow: New evidence for atmospheric formation. *Environmental Science and Technology*, 05, 3455-3461.

Zhang, F., Yang, X., Xue, X., Tao, X., Lu, G., & Dang, Z. (2013). Estimation of n-octanol/water partition coefficients (logKow) of polychlorinated biphenyls by using quantum chemical descriptors and partial least squares. *Journal of Chemistry*, 213.

Zhang, Z. L. (2003). Studies on the sea surface microlayer: II. The layer of sudden change of physical and chemical properties. *Journal of Colloid and Interface Science*, 246(1), 148-159.

Zhao, C., Boriani, e., Chana, E., Roncaglioni, A., & Benfenati, E. (2008). A New Hybrid QSAR Model for Predicting Bioconcentration Factor (BCF). *Chemosphere*, 73, 1701-1707.

Zhou, W., Zhai, Z., Wang, Z., & Wang, L. (2005). Estimation of n-octanol/water parition coefficients (KOW) of all PCB congeners by density functional theory. *Journal of Molecular Structure:* Thermochem, 755, 137-145.

Zitko, V. C. (2000). *Ultraviolet spectra of water from the Miramichi watershed. In Canadian Technical Report of Hydrography and Ocean Sciences*, 2302, 1–30. New Brunswick.

Zuev, B. K. (2001). Conditions of formation of the chemical microlayer and techniques for studying organic matter in it. *Geochemistry International*, 39, 773-784.

Appendices

Table S.1 Molecular polarizability calculated with B3LYP functionals and the 6-311g(d,p) basis set

Compound	α_{xx}	α_{yy}	α_{zz}	Average	Polarizability (Å^3)
Chloroethene (Vinyl chloride)	45.254	42.726	27.004	38.328	5.6796
1,1-Dichloroethene	58.142	60.979	33.713	50.945	7.5493
cis-1,2-Dichloroethene	62.492	55.805	33.564	50.62	7.5011
trans-1,2-Dichloroethene	57.678	65.417	33.567	52.221	7.7384
Trichloroethylene	67.822	86.205	40.426	64.818	9.6050
Tetrachloroethylene	90.251	97.547	47.386	78.395	11.617
1,3-Dichloropropene	98.685	51.814	50.842	67.114	9.9453
Chloroprene	81.875	69.27	40.581	63.909	9.4703
Hexachlorobutadiene	159.553	124.317	115.604	133.158	19.732
Hexachlorocyclopentadiene	69.652	69.637	59.148	66.146	9.8018
Pentachlorotoluene	191.349	181.439	83.795	152.194	22.553
Fluorobenzene	81.376	78.773	41.892	67.347	9.9798
1,2-Difluorobenzene	82.443	79.336	40.973	67.584	10.050
1,3-Difluorobenzene	82.434	79.329	40.972	67.578	10.014
1,4-Difluorobenzene	40.798	78.291	82.949	67.346	9.9796
1,2,4-Trifluorobenzene	83.993	79.479	40.208	67.893	10.061
1,3,5-Trifluorobenzene	82.443	79.336	40.973	67.584	10.015
1,2,3,4-Tetrafluorobenzene	84.277	81.713	39.805	68.598	10.165
1,2,3,5-Tetrafluorobenzene	84.046	81.907	39.703	68.552	10.158
1,2,4,5-Tetrafluorobenzene	85.853	79.837	39.545	68.412	10.138
Pentafluorobenzene	85.612	82.906	39.263	69.26	10.263
Hexafluorobenzene	38.921	85.677	85.674	70.091	10.386
Benzotrifluoride	100.757	88.734	53.405	80.965	11.998
Chloropentafluorobenzene	113.868	92.023	46.362	84.084	12.460
Fluoromethane	14.956	14.956	16.197	15.37	2.2776
Difluoromethane	15.045	17.409	16.037	16.164	2.3953
Trifluoromethane	17.693	17.692	16.063	17.149	2.5412
Tetrafluoromethane	17.792	17.792	17.792	17.792	2.6365
Chlorofluoromethane	27.036	32.331	22.875	27.414	4.0623
Dichlorofluoromethane	32.612	37.459	52.032	40.701	6.0313
Chlorodifluoromethane	30.771	29.265	25.807	28.614	4.2402
Chlorotrifluoromethane	26.021	26.018	35.469	29.169	4.3224
Dichlorodifluoromethane	51.265	33.99	38.994	41.416	6.1372
Trichlorofluoromethane	59.349	59.354	43.415	54.039	8.0078
Fluoroethane	29.001	27.272	25.671	27.315	4.0477
1,1-Difluoroethane	29.003	28.281	26.627	27.97	4.1447
1,2-Difluoroethane	27.843	29.341	25.343	27.509	4.0764
1,1,2-Trichloro-1,2,2-trifluoroethane	64.986	70.874	63.475	66.445	9.8461

1,1,2,2-Tetrachloro-1,2-difluoroethane	82.986	77.671	78.063	79.573	11.792
1-Chloro-2-fluoroethane	48.959	36.105	33.02	39.361	5.8327
1-Chloro-1,1-difluoroethane	48.627	37.311	36.186	40.708	6.0323
1-Chloro-1,1,2-trifluoroethane	42.989	43.742	36.865	41.199	6.1051
1-Chloro-1,2,2,2-tetrafluoroethane	47.068	41.033	37.03	41.71	6.1808
1-Chloropentafluoroethane	46.49	42.597	38.946	42.678	6.3242
1,1-Dichloro-1-fluoroethane	62.338	53.064	44.607	53.336	7.9036
1,2-Dichloro-1,1-difluoroethane	72.914	47.746	44.987	55.216	8.1822
1,1-Dichlorotrifluoroethane	43.979	53.258	64.022	53.753	7.9654
1,2-Dichloro-1,1,2,2-tetrafluoroethane	57.225	57.689	48.303	54.406	8.0621
1,1-Dichloro-1,2,2,2-tetrafluoroethane	52.949	63.777	47.875	54.867	8.1305
1,1,1-Trichloro-2,2,2-trifluoroethane	59.498	71.163	71.161	67.274	9.969
1,1,2-Trichloro-1,2,2-trifluoroethane	64.986	70.874	63.475	66.445	9.8461
1,1-Difluorotetrachloroethane	82.986	77.671	78.063	79.573	11.792
1,1,2,2-Tetrachloro-1,2-difluoroethane	83.566	94.058	62.398	80.007	11.856
1-chloro-2,2-difluoroethane	47.108	37.245	35.901	40.085	5.9400
1,1,1,2-Tetrofluoroethane	29.834	29.107	28.067	29.003	4.2978
Perfluoroethane	30.503	31.014	31.011	30.843	4.5705
1,1,1,2,2-Pentachloro-2-fluoroethane	90.568	100.711	84.479	91.919	13.621
Fluoropropane	75.075	59.85	55.303	63.409	9.3962
2-Fluoropropane	42.275	39.123	37.011	39.47	5.8489
1,1,2,2,3-Pentafluoropropane	41.442	41.413	40.687	41.181	6.1024
1,1,1,3,3-Pentafluoropropane	44.171	40.295	38.644	41.037	6.0811
1,1,1,2,2-Pentafluoropropane	41.496	41.523	40.395	41.138	6.0960
1,1,1,2,3,3-Hexafluoropropane	44.427	42.426	39.056	41.97	6.2193
1,1,1,3,3,3-Hexafluoropropane	44.444	40.087	40.597	41.709	6.1806
1,1,1,2,3,3,3-Heptafluoropropane	42.275	39.123	37.011	39.47	5.8489
Octafluoropropane	45.271	42.731	43.284	43.762	6.4849
Perfluorobutane	54.947	60.311	55.215	56.824	8.4204
Perfluorocyclobutane	44.821	42.6	40.811	42.744	6.3340
Perfluoropentane	75.898	66.733	66.363	69.665	10.323
Bromomethane	42.728	28.907	28.907	33.514	4.9663
Dibromomethane	75.094	46.822	42.475	54.797	8.1201
Tribromomethane	86.971	86.954	56.141	76.689	11.364
Bromoethane	59.701	42.155	39.816	47.224	6.9979
1,2-Dibromoethane	103.306	55.593	53.277	70.725	10.480
1-Bromopropane	78.149	52.434	49.754	60.112	8.9077
2-Bromopropane	73.666	57.143	50.736	60.515	8.9674
1,2-Dibromopropane	114.361	72.038	64.041	83.48	12.3705
1-Bromobutane	92.92	62.995	61.159	72.358	10.722
1-Bromopentane	84.393	97.562	68.475	83.477	12.37
1-Bromohexane	115.932	91.945	81.791	96.556	14.308
1-Bromoheptane	147.698	96.43	88.275	110.801	16.419

1-Bromooctane	138.352	119.15	103.399	120.3	17.827
1-Bromodecane	200.304	128.594	117.331	148.743	22.041
1-Bromododecane	236.064	149.638	136.489	174.064	25.794
Bromocyclohexane	115.126	85.519	76.386	92.344	13.684
Vinyl bromide	64.616	40.14	33.074	45.943	6.8081
Bromochloromethane	63.453	41.01	36.564	47.009	6.9660
Bromodichloromethane	53.892	64.126	64.913	60.977	9.0359
Dibromochloromethane	82.073	73.407	50.912	68.797	10.195
Bromobenzene	123.95	90.283	55.233	89.822	13.310
1,2-Dibromobenzene	142.3	123.253	66.839	110.797	16.418
1,3-Dibromobenzene	156.602	116.442	67.444	113.496	16.818
1,4-Dibromobenzene	174.162	101.137	67.51	114.27	16.933
1,2,3-Tribromobenzene	169.952	150.118	78.305	132.792	19.678
1,2,4-Tribromobenzene	192.698	136.668	79.009	136.125	20.172
1,3,5-Tribromobenzene	167.462	167.402	79.59	138.151	20.472
1,2,4,5-Tetrabromobenzene	221.485	166.266	90.463	159.405	23.621
Hexabromobenzene	246.174	246.161	111.471	201.269	29.825
2-Bromotoluene	133.623	109.738	63.799	102.387	15.172
3-Bromotoluene	138.72	108.11	64.261	103.697	15.366
4-Bromotoluene	148.808	99.17	64.255	104.078	15.423
2-Bromochlorobenzene	131.926	115.605	61.238	102.923	15.252
4-bromodiphenyl ether 3	245.286	141.412	120.871	169.19	25.071
2,4-dibromodiphenyl ether 7	251.092	185.902	137.605	191.533	28.382
2,4'-dibromodiphenyl ether 8	264.257	175.966	137.42	192.548	28.533
di(4-Bromophenyl)ether 15	297.062	159.566	130.268	195.632	28.990
2,4-Dibromo-1-(2-bromophenoxy)benzene 17	262.034	196.915	178.232	212.394	31.474
2,4-Dibromo-1-(4-bromophenoxy)benzene 28	308.966	201.075	146.979	219.007	32.454
2,4,6-Tribromo-diphenyl ether 30	280.513	200.765	155.733	212.337	31.465
2,6-Dibromo-1-(4-bromophenoxy)benzene 32	264.767	201.75	166.063	210.86	31.246
3,4-Dibromo-1-(3-bromophenoxy)benzene 35	325.905	176.162	154.251	218.773	32.419
bis(2,4-dibromophenyl) ether 47	318.684	216.909	184.02	239.871	35.545
bis(3,4-dibromophenyl) ether 77	363.284	198.436	166.885	242.868	35.989
1,2,3-Tribromo-4-(2,4-dibromophenoxy)benzene 85	356.964	229.966	196.052	260.994	38.675
2,2′,4,4′,5-Pentabromodiphenyl ether 99	329.153	258.209	195.838	261.067	38.686
1,3,5-Tribromo-2-(2,4-dibromophenoxy)benzene 100	337.887	222.67	222.956	261.171	38.702
1,1'-Oxybis(2,4,5-tribromobenzene) 153	347.961	284.225	228.143	286.776	42.496
1,3,5-Tribromo-2-(2,4,5-tribromophenoxy)benzene 154	397.256	236.583	220.487	284.775	42.199
1,2,3,5-Tetrabromo-4-(2,4,5-tribromophenoxy)benzene 183	373.92	278.207	262.063	304.73	45.156

1,4-Dioxane	62.059	52.956	50.056	55.024	8.1537
2,4,5'-Trichlorobiphenyl	200.295	285.11	95.15	193.518	28.676
2,2',4,5'-Tetrachlorobiphenyl 49	224.036	299.454	101.495	208.328	30.871
2,3,4,5,6-Pentachlorobiphenyl 116	107.959	240.894	316.903	221.919	32.885
2,3,3',4,4'-Pentachlorobiphenyl 121	282.663	288.633	107.952	226.416	33.551
2,2',4,5,5'-Pentachlorobiphenyl 101	264	298.134	107.928	223.354	33.098
2,2',3,4,5'-Pentachlorobiphenyl 87	299.406	259.875	107.862	222.381	32.954
2,2',4,5',6-Pentachlorobiphenyl 103	276.762	179.322	176.48	210.855	31.246
2,2',4,6,6'-Pentachlorobiphenyl 104	107.938	253.183	302.07	221.064	32.758
2,3',4,4',6-Pentachlorobiphenyl 119	257.31	315.834	107.975	227.04	33.644
3,3',4,4',5-Pentachlorobiphenyl 126	257.018	257.018	107.933	207.323	30.722
2,3',4,4',5-Pentachlorobiphenyl 123	223.573	351.401	107.977	227.65	33.734
p,p'-DDE	114.399	338.837	271.449	241.562	35.796
1,2,3,4-Tetrachlorobenzene	166.868	136.92	68.501	124.096	18.389
1,2,3,4-Tetrabromo-5-chloro-6-methylbenzene	232.191	215.76	103.981	183.977	27.263
Pentabromotoluene	243.368	224.324	108.862	192.185	28.479
3-Chlorobenzotrifluoride	122.261	104.676	59.948	95.628	14.171
4,4′-dibromobiphenyl	328.658	157.683	109.06	198.467	29.410
1,2,3,4-Tetrachloronaphthalene	241.932	202.754	89.145	177.944	26.369
Hexachlorobutadiene	159.553	124.322	115.597	133.157	19.732
1-Chlorobutane	81.129	58.277	53.201	64.202	9.5138
1,10-Dibromodecane	241.568	143.572	130.719	171.953	25.481
1,1,2,2-Tetrabromoethane	123.59	108.491	97.792	109.958	16.294
tetra(bromomethyl)methane	172.713	128.703	132.894	144.77	21.453
1,1-Dichloroethene	58.167	60.985	33.715	50.956	7.5509
Allyl chloride	70.982	42.49	43.709	52.394	7.7640

Table S.2 Compounds used to correlate molecular polarizability and log K_{OW}, predicted results are indicated.

Compound	Polarizability ($Å^3$)	Training Set	Validation Set	Predicted *log* K_{ow}	Measured *log* K_{ow}	Standard error of measurements
Benzene	9.81	√		2.72	2.13	
Chlorobenzene	10.4825	√		2.83	2.82	0.07
1,2-Dichlorobenzene	12.1401	√		3.10	3.48	0.04
1,3-Dichlorobenzene	12.302	√		3.13	3.50	0.02
1,4-Dichlorobenzene	12.3496	√		3.14	3.44	0.04
1,2,3-Trichlorobenzene	13.8846	√		3.39	4.09	0.03
1,2,4-Trichlorobenzene	14.1106		√	3.43	4.04	0.04
1,3,5-Trichlorobenzene	14.2183	√		3.45	4.20	0.05
1,2,3,4-Tetrachlorobenzene	15.7488	√		3.70	4.58	0.05
1,2,3,5-Tetrachlorobenzene	15.9196	√		3.73	4.62	0.06
1,2,4,5-Tetrachlorobenzene	15.9804	√		3.74	4.63	0.05
Pentachlorobenzene	17.7032		√	4.02	5.07	0.06
Hexachlorobenzene	19.4794	√		4.31	5.36	0.1
Naphthalene	15.72	√		3.69	3.36	0.009
1-Chloronaphthelene	17.4469	√		3.98	3.90	*
2-Chloronaphthelene	17.8037		√	4.04	3.98	*
1,2-Dichloronaphthelene	19.4428	√		4.31	4.42	*
1,3-Dichloronaphthelene	19.5916			4.33		
1,4-Dichloronaphthelene	19.3249		√	4.29	4.66	*
1,5-Dichloronaphthelene	19.2571			4.28		
1,6-Dichloronaphthelene	19.6127			4.34		
1,7-Dichloronaphthelene	19.5588			4.33		
1,8-Dichloronaphthelene	19.2398	√		4.27	4.19	*
2,3-Dichloronaphthelene	19.7973	√		4.37	4.51	*
2,6-Dichloronaphthelene	20.0301			4.40		
2,7-Dichloronaphthelene	20.001	√		4.40	4.56	*
1,2,3-Trichloronaphthelene	21.49112			4.65		
1,2,4-Trichloronaphthelene	21.35083			4.62		
1,2,5-Trichloronaphthelene	21.31546			4.62		
1,2,6-Trichloronaphthelene	21.74613			4.69		
1,2,7-Trichloronaphthelene	21.65819			4.67		
1,2,8-Trichloronaphthelene	21.26122			4.61		
1,3,5-Trichloronaphthelene	21.42735			4.64		
1,3,6-Trichloronaphthelene	21.87131			4.71		
1,3,7-Trichloronaphthelene	21.84725	√		4.70	5.35	*
1,3,8-Trichloronaphthelene	21.45422			4.64		
1,4,5-Trichloronaphthelene	21.18766			4.60		

1,4,6-Trichloronaphthelene	21.49083			4.65		
1,6,7-Trichloronaphthelene	21.62233			4.67		
2,3,6-Trichloronaphthelene	22.12809			4.75		
Biphenyl	19.05	√		4.24	3.86	0.08
2-Chlorobiphenyl (PCB-1)	20.3357	√		4.46	4.51	0.03
4-Chlorobiphenyl (PCB-3)	21.2568		√	4.61	4.49	0.07
2,2'-Chlorobiphenyl (PCB-4)	21.5545	√		4.66	4.92	0.04
2,3-Chlorobiphenyl (PCB-5)	22.1178			4.75		
2,3'-Chlorobiphenyl (PCB-6)	22.1858			4.76		
2,4-Chlorobiphenyl (PCB-7)	22.5566			4.82		
2,4'-Chlorobiphenyl (PCB-8)	22.4658	√		4.81	5.12	0.02
2,5-Chlorobiphenyl (PCB-9)	22.3437	√		4.79	5.16	*
2,6-Chlorobiphenyl (PCB-10)	21.6091	√		4.67	4.96	0.03
3,3'-Chlorobiphenyl (PCB-11)	22.8207	√		4.87	5.30	*
3,4-Chlorobiphenyl (PCB-12)	23.0621		√	4.91	5.29	*
3,4'-Chlorobiphenyl (PCB-13)	23.2044			4.93		
3,5-Chlorobiphenyl (PCB-14)	22.9312	√		4.88	5.37	*
4,4'-Chlorobiphenyl (PCB-15)	23.5603	√		4.99	5.44	0.06
2,3,2'-Trichlorobiphenyl (PCB-16)	23.33029			4.95		
2,4,2'-Trichlorobiphenyl (PCB-17)	23.64472	√		5.00	5.50	*
2,6,2'-Trichlorobiphenyl (PCB-18)	23.12419		√	4.92	5.71	0.2
2,3,3'-Trichlorobiphenyl (PCB-20)	23.98538	√		5.06	5.68	*
2,3,4-Trichlorobiphenyl (PCB-21)	24.19054		√	5.09	5.86	*
2,3,4'-Trichlorobiphenyl (PCB-22)	24.29699	√		5.11	5.63	*
2,3,5-Trichlorobiphenyl (PCB-23)	24.18249			5.09		
2,3,6-Trichlorobiphenyl (PCB-24)	23.5559			4.99		
2,4,3'-Trichlorobiphenyl (PCB-25)	24.45097			5.13		
2,5,3'-Trichlorobiphenyl (PCB-26)	24.214			5.10		
2,6,3'-Trichlorobiphenyl (PCB-27)	23.4729			4.97		
2,4,4'-Trichlorobiphenyl (PCB-28)	24.7784	√		5.19	5.23	0.4
2,4,5-Trichlorobiphenyl (PCB-29)	24.45023		√	5.13	5.77	0.09
2,4,6-Trichlorobiphenyl (PCB-30)	23.79682	√		5.03	5.63	0.06
2,5,4'-Trichlorobiphenyl (PCB-31)	24.04501	√		5.07	5.79	*
2,6,4'-Trichlorobiphenyl (PCB-32)	23.64121	√		5.00	5.47	*
3,4,2'-Trichlorobiphenyl (PCB-33)	23.77958	√		5.02	5.87	*
2,3,5'-Trichlorobiphenyl (PCB-34)	24.02282			5.06		
3,4,3'-Trichlorobiphenyl (PCB-35)	24.99927			5.22		
3,3',5-Trichlorobiphenyl (PCB-36)	24.83906			5.20		
3,4,4'-Trichlorobiphenyl (PCB-37)	25.42732			5.30		
3,5,4'-Trichlorobiphenyl (PCB-39)	25.24562			5.27		
2,3,2',3'-Tetrachlorobiphenyl (PCB-40)	25.17829	√		5.25	5.84	0.2
2,3,2',4'-Tetrachlorobiphenyl (PCB-42)	25.50695			5.31		
2,3,4,2'-Tetrachlorobiphenyl (PCB-41)	25.34516			5.28		
2,3,5,2'-Tetrachlorobiphenyl (PCB-43)	25.4206			5.29		

2,3,2',5'-Tetrachlorobiphenyl (PCB-44)	25.38676			5.29		
2,3,6,2'-Tetrachlorobiphenyl (PCB-45)	25.06344			5.24		
2,3,2',6'-Tetrachlorobiphenyl (PCB-46)	24.91943			5.21		
2,4,5,2'-Tetrachlorobiphenyl (PCB-47)	25.84998	√		5.37	5.68	*
2,4,2',4'-Tetrachlorobiphenyl (PCB-48)	25.57897	√		5.32	6.05	0.3
2,2',4,6'-Tetrachlorobiphenyl (PCB-51)	25.26454			5.27		
2,5,2',5'-Tetrachlorobiphenyl (PCB-52)	25.57981	√		5.32	5.81	*
2,5,2',6'-Tetrachlorobiphenyl (PCB-53)	25.13102	√		5.25	5.46	*
2,6,2',6'-Tetrachlorobiphenyl (PCB-54)	24.7374	√		5.18	5.71	0.2
2,3,4,3'-Tetrachlorobiphenyl (PCB-55)	26.06398			5.40		
2,3,3',4'-Tetrachlorobiphenyl (PCB-56)	26.04037			5.40		
2,3,4,4'-Tetrachlorobiphenyl (PCB-60)	26.44392			5.46		
2,3,4,5-Tetrachlorobiphenyl (PCB-61)	26.15715			5.42		
2,3,4',5-Tetrachlorobiphenyl (PCB-63)	26.41393			5.46		
2,3,4',6-Tetrachlorobiphenyl (PCB-64)	25.62526			5.33		
2,3,5,6-Tetrachlorobiphenyl (PCB-65)	25.55981		√	5.32	5.94	*
2,4,3',4'-Tetrachlorobiphenyl (PCB-66)	26.56663		√	5.48	6.20	0.1
2,3',4,5-Tetrachlorobiphenyl (PCB-67)	26.37599			5.45		
2,3',4,6-Tetrachlorobiphenyl (PCB-69)	25.69842			5.34		
2,5,3',4'-Tetrachlorobiphenyl (PCB-70)	26.31429	√		5.44	5.99	*
2,6,3',4'-Tetrachlorobiphenyl (PCB-71)	25.4285			5.30		
2,5,3',5'-Tetrachlorobiphenyl (PCB-72)	26.17311			5.42		
2,4,5,4'-Tetrachlorobiphenyl (PCB-74)	26.71601			5.51		
2,4,6,4'-Tetrachlorobiphenyl (PCB-75)	25.88955			5.37		
3,4,3',4'-Tetrachlorobiphenyl (PCB-77)	27.25507	√		5.60	6.36	0.1
3,4,5,3'-Tetrachlorobiphenyl (PCB-78)	26.89262			5.54		
3,4,3',5'-Tetrachlorobiphenyl (PCB-79)	27.05109			5.56		
3,5,3',5'-Tetrachlorobiphenyl (PCB-80)	26.85512			5.53		
3,4,5,4'-Tetrachlorobiphenyl (PCB-81)	27.34789		√	5.61	6.53	*
Methane	2.11941			1.45		
Monochloromethane	3.54598	√		1.69	0.91	*
Dichloromethane	5.2984	√		1.97	1.25	*
Trichloromethane	7.22831	√		2.29	1.92	0.02
Tetrachloromethane	9.12655	√		2.61	2.73	0.04
Ethane	3.91767			1.75		
Monochloroethane	5.5283	√		2.01	1.43	*
1,1-Dichloroethane	7.35887		√	2.31	1.79	*
1,1,1-Trichloroethane	9.24654	√		2.63	2.48	0.007
1,2-Dichloroethane	7.34642	√		2.31	1.47	0.02
1,1,1-Trichloroethane	9.80000		√	2.72	2.49	0.01
1,1,2-Trichloroethane	9.11865	√		2.60	1.89	*
1,1,1,2-Tetrachloroethane	10.96245			2.91		
1,1,2,2-Tetrachloroethane	10.84078	√		2.89	2.39	0
Pentachloroethane	12.74994		√	3.20	2.89	*

Hexachloroethane	14.55235	√		3.50	3.93	*
Propane	5.7179			2.04		
1-Monochloropropane	7.38476	√		2.32	2.04	*
1,1-Dichloropropane	9.18662			2.62		
1,1,1-Trichloropropane	11.03359			2.92		
2-Monochloropropane	7.4799		√	2.33	1.90	*
1,2-Dichloropropane	9.11069			2.60		
1,1,2-Trichlororpropane	10.85115			2.89		
1,1,1,2-Tetrachloropropane	12.77138			3.21		
2,2-Dichloropropane	9.32692			2.64		
1,2,2-Trichloropropane	10.91251			2.90		
1,1,2,2-Tetrachloropropane	12.74703			3.20		
1,1,1,2,2-Pentachloropropane	14.54361			3.50		
1,3-Dichloropropane	9.12329			2.61		
1,1,3-Trichloropropane	10.96907			2.91		
1,1,1,3-Tetrachloropropane	12.83338			3.22		
1,2,3-Trichloropropane	10.79336			2.88		
1,1,2,3-Tetrachloropropane	12.73063			3.20		
1,2,2,3-Tetrachloropropane	12.56484			3.17		
1,1,2,2,3-Pentachloropropane	14.46615			3.49		
1,1,1,2,2,3-Hexachloropropane	16.27987			3.79		
1,1,3,3-Tetrachloropropane	12.76303			3.21		
1,1,2,3,3-Pentachloropropane	14.49243			3.49		
1,1,1,2,2,3,3-Heptachloropropane	18.0929			4.09		
1,1,3,3,3-Pentachloropropane	14.53308			3.50		
1,1,2,3,3,3-Hexachloropropane	16.35328			3.80		
1,1,1,2,3,3,3-Heptachloropropane	18.09226			4.09		
Octachloropropane	19.84813			4.37		
Chloroethene (Vinyl chloride)	5.68			2.04		
1,1-Dichloroethene	7.55	√		2.35	2.13	
cis-1,2-Dichloroethene	7.5	√		2.34	1.86	
trans-1,2-Dichloroethene	7.74	√		2.38	2.09	
Trichloroethylene	9.6		√	2.68	2.42	0
Tetrachloroethylene	11.62	√		3.02	3.00	0.4
1,3-Dichloropropene	9.95			2.74		
Chloroprene	9.47	√		2.66	2.03	
Hexachlorobutadiene	19.73		√	4.36	4.78	
2-Chlorotoluene	13.96	√		3.40	3.42	*
3-Chlorotoluene	14.09		√	3.42	3.28	0
4-Chlorotoluene	14.14	√		3.43	3.32	0.02
2,3-Dichlorotoluene	16.03			3.74		
2,4-Dichlorotoluene	16.23	√		3.78	4.24	*
2,5-Dichlorotoluene	16.24			3.78		
2,6-Dichlorotoluene	16.05			3.75		

3,4-Dichlorotoluene	16.18			3.77		
3,5-Dichlorotoluene	16.34			3.80		
2,3,6-Trichlorotoluene	18.22			4.11		
2,4,5-Trichlorotoluene	18.41			4.14		
a-HCH	18.63		√	4.17	3.79	0.02
b-HCH	19.26	√		4.28	3.81	0.02
c-HCH	18.84	√		4.21	4.14	*
p,p'-DDT	30.76	√		6.18	6.91	0.3
Pentachlorotoluene	22.55			4.82		
Fluorobenzene	9.98	√		2.75	2.27	
1,2-Difluorobenzene	10.01			2.75	2.37	**0.13
1,3-Difluorobenzene	7.51			2.34	2.58	**0.14
1,4-Difluorobenzene	9.98			2.75	2.48	**0.21
1,2,4-Trifluorobenzene	10.06			2.76	2.52	**0.08
1,3,5-Trifluorobenzene	9.78			2.71		
1,2,3,4-Tetrafluorobenzene	10.17			2.78		
1,2,3,5-Tetrafluorobenzene	10.16			2.78		
1,2,4,5-Tetrafluorobenzene	10.14			2.77		
Pentafluorobenzene	10.26	√		2.79	2.53	
Hexafluorobenzene	10.39	√		2.81	2.54	
Benzotrifluoride	10.52		√	2.84	3	
Chloropentafluorobenzene	12.47			3.16		
Fluoromethane	2.28			1.48	0.51	**
Difluoromethane	2.10			1.45	0.20	**
Trifluoromethane	2.54			1.52	0.64	**
Tetrafluoromethane	2.64			1.54	1.18	**
Chlorofluoromethane	4.06			1.77	1.55	**
Dichlorofluoromethane	6.03			2.09	1.55	**
Chlorodifluoromethane	4.24			1.80	1.08	**
Chlorotrifluoromethane	4.32			1.81	1.65	**
Dichlorodifluoromethane	6.14		√	2.11	2.16	
Trichlorofluoromethane	8.01	√		2.42	2.53	
Fluoroethane	4.05		√	1.77	1.24	
1,1-Difluoroethane	4.14	√		1.78	0.75	
1,2-Difluoroethane	4.08	√		1.77	0.75	
1,1,2-Trichloro-1,2,2-trifluoroethane	9.85			2.73	3.16	**
1,1,2,2-Tetrachloro-1,2-difluoroethane	11.9			3.06	2.82	**
1-Chloro-2-fluoroethane	5.83			2.06		
1-Chloro-1,1-difluoroethane	6.02			2.09	1.6	**
1-Chloro-1,1,2-trifluoroethane	6.11			2.11		
1-Chloro-1,2,2,2-tetrafluoroethane	6.18			2.12	1.867	**
1-Chloropentafluoroethane	6.32			2.14	2.3	**
1,1-Dichloro-1-fluoroethane	7.9			2.40	2.04	**
1,2-Dichloro-1,1-difluoroethane	8.18			2.45		

1,1-Dichlorotrifluoroethane	7.97			2.42		
1,2-Dichloro-1,1,2,2-tetrafluoroethane	8.06			2.43	2.82	**
1,1-Dichloro-1,2,2,2-tetrafluoroethane	8.13			2.44	2.85	**
1,1,1-Trichloro-2,2,2-trifluoroethane	9.97			2.75		
1,1,2-Trichloro-1,2,2-trifluoroethane	9.85			2.73	3.16	**
1,1-Difluorotetrachloroethane	11.79			3.05	2.85	**
1,1,2,2-Tetrachloro-1,2-difluoroethane	11.86			3.06	2.82	**
1-chloro-2,2-difluoroethane	5.94			2.08	1.6	**
1,1,1,2-Tetrofluoroethane	4.3			1.81	1.06	**
Perfluoroethane	4.57			1.85	2	**
1,1,1,2,2-Pentachloro-2-fluoroethane	13.62			3.35		
Fluoropropane	9.40		√	2.65	2.33	
2-Fluoropropane	5.85			2.07		
1,1,2,2,3-Pentafluoropropane	6.10			2.11		
1,1,1,3,3-Pentafluoropropane	6.08			2.10		
1,1,1,2,2-Pentafluoropropane	6.12			2.11		
1,1,1,2,3,3-Hexafluoropropane	6.22			2.13		
1,1,1,3,3,3-Hexafluoropropane	6.18			2.12		
1,1,1,2,3,3,3-Heptafluoropropane	6.33			2.14		
Octafluoropropane	6.48			2.17		
Perfluorobutane	8.41			2.49		
Perfluorocyclobutane	6.44			2.16		
Perfluoropentane	10.32			2.80		
Bromomethane	4.97		√	1.92	1.19	
Dibromomethane	8.12	√		2.44	1.88	
Tribromomethane	11.36	√		2.974	2.67	
Bromoethane	7	√		1.78	1.61	
1,2-Dibromoethane	10.48	√		2.83	1.96	
1-Bromopropane	8.91	√		2.57	2.1	
2-Bromopropane	8.97		√	2.58	2.14	
1,2-Dibromopropane	12.37			3.14		
1-Bromobutane	10.72	√		2.87	2.75	
1-Bromopentane	12.37		√	3.14	3.37	
1-Bromohexane	14.31	√		3.46	3.8	
1-Bromoheptane	16.42	√		3.81	4.36	
1-Bromooctane	17.83	√		4.04	4.89	
1-Bromodecane	22.04			4.74		
1-Bromododecane	25.79			5.35		
Bromocyclohexane	13.68		√	3.36	3.2	
Vinyl bromide	6.81	√		2.22	1.57	
Bromochloromethane	6.97	√		2.25	1.41	
Bromodichloromethane	9.04		√	2.59	2	
Dibromochloromethane	10.19	√		2.78	2.16	
Bromobenzene	13.31	√		3.30	2.923	0.1

1,2-Dibromobenzene	16.42		√	3.81	3.64	
1,3-Dibromobenzene	16.82	√		3.87	3.77	0.02
1,4-Dibromobenzene	16.93	√		3.89	3.77	0.02
1,2,3-Tribromobenzene	19.68			4.35		
1,2,4-Tribromobenzene	20.17	√		4.43	4.51	
1,3,5-Tribromobenzene	20.47	√		4.48	4.51	
1,2,4,5-Tetrabromobenzene	23.62		√	5.00	5.13	
Hexabromobenzene	29.82			6.02		
2-Bromotoluene	15.17			3.60		
3-Bromotoluene	15.37			3.64		
4-Bromotoluene	15.42			3.64		
2-Bromochlorobenzene	15.25			3.62		
4-bromodiphenyl ether 3	25.0714			5.24		**
2,4-dibromodiphenyl ether 7	28.3823			5.78		**
2,4'-dibromodiphenyl ether 8	28.5327			5.81		**
di(4-Bromophenyl)ether 15	28.9897			5.88		**
2,4-Dibromo-1-(2-bromophenoxy)benzene 17	31.4735	√		6.29	5.74	*
2,4-Dibromo-1-(4-bromophenoxy)benzene 28	32.4535		√	6.45	5.94	0.15
2,4,6-Tribromo-diphenyl ether 30	31.4651			6.29		**
2,6-Dibromo-1-(4-bromophenoxy)benzene 32	31.2462			6.26		**
3,4-Dibromo-1-(3-bromophenoxy)benzene 35	32.4188			6.44		**
bis(2,4-dibromophenyl) ether 47	35.5452	√		6.97	6.81	0.08
bis(3,4-dibromophenyl) ether 77	35.9893			7.04		
1,2,3-Tribromo-4-(2,4-dibromophenoxy)benzene 85	38.6753	√		7.48	7.37	0.12
2,2′,4,4′,5-Pentabromodiphenyl ether 99	38.6861	√		7.48	7.32	0.14
1,3,5-Tribromo-2-(2,4-dibromophenoxy)benzene 100	38.7015		√	7.52	7.24	0.16
1,1'-Oxybis(2,4,5-tribromobenzene) 153	42.4958	√		8.11	7.9	0.14
1,3,5-Tribromo-2-(2,4,5-tribromophenoxy)benzene 154	42.1993	√		8.06	7.82	0.16
1,2,3,5-Tetrabromo-4-(2,4,5-tribromophenoxy)benzene 183	45.1563	√		8.55	8.27	0.26

Note:
Polarizability data with 2 decimal places are reproduced from Staikova et al. (2005) and Staikova et al. (2004), data with 4 decimal places are calculated by this research.
* Single measurement only. Standard error assumed as 0.3.
** *log* K_{OW} data from other models, standard error assumed as 0.3 if not specified.

Table S.3 Compounds used to correlating molecular polarizability and log BCF, predicted results are indicated.

Compound	Polarizability (Å^3)	Fish BCF	Predicted *log BCF*
Chlorobenzene	10.4825	1.13	1.45
1,2-Dichlorobenzene	12.1401	2.24	1.70
1,3,5-Trichlorobenzene	14.2183	2.97	2.01
1,2,3-Trichlorobenzene	13.8846	2.82	1.96
1,2,3,4-Tetrachlorobenzene	15.7488	3.04	2.25
Pentachlorobenzene	17.7032	3.49	2.54
2,2'-Chlorobiphenyl (PCB-4)	21.5545	3.53	3.13
2,3-Chlorobiphenyl (PCB-5)	22.1178	3.72	3.21
3,5-Chlorobiphenyl (PCB-14)	22.9312	3.11	3.33
2,4,2'-Trichlorobiphenyl (PCB-17)	23.64472	4.17	3.44
2,4,5-Trichlorobiphenyl (PCB-29)	24.45023	4.22	3.57
2,3,2',3'-Tetrachlorobiphenyl (PCB-40)	25.17829	4.17	3.68
2,3,2',4'-Tetrachlorobiphenyl (PCB-42)	25.50695	4.53	3.73
2,5,2',5'-Tetrachlorobiphenyl (PCB-52)	25.57981	4.44	3.74
2,3,4,5-Tetrachlorobiphenyl (PCB-61)	26.15715	4.39	3.82
2,4,3',4'-Tetrachlorobiphenyl (PCB-66)	26.56663	4.56	3.89
2,5,3',5'-Tetrachlorobiphenyl (PCB-72)	26.17311	4.85	3.83
3,4,3',4'-Tetrachlorobiphenyl (PCB-77)	27.25507	3.51	3.99
2,5,4'-Trichlorobiphenyl (PCB-31)	24.04501	3.95	3.50
2,2',4,5'-Tetrachlorobiphenyl (PCB- 49)	30.8710	4.26	4.54
2,3,4,5,6-Pentachlorobiphenyl (PCB-116)	32.8850	4.85	4.84
2,2',4,5',6-Pentachlorobiphenyl (PCB- 103)	31.2455	4.58	4.60
2,3,3',4,4'-Pentachlorobiphenyl (PCB-121)	33.5514	4.81	4.96
2,2',4,5,5'-Pentachlorobiphenyl (PCB-101)	33.0976	4.63	4.88
2,2',3,4,5'-Pentachlorobiphenyl (PCB-87)	32.9535	4.02	4.85
3,3',4,4',5-Pentachlorobiphenyl (PCB-126)	30.7221	4.68	4.52
2,3',4,4',6-Pentachlorobiphenyl (PCB- 119)	33.6439	4.81	4.96
2,3',4,4',5-Pentachlorobiphenyl (PCB- 123)	33.7342	4.38	4.97
2,2',4,6,6'-Pentachlorobiphenyl (PCB- 104)	32.7583	4.81	4.83
Dichloromethane	5.2984	1.37	0.66
Tetrachloromethane	9.12655	0.87	1.24
1,1,2-Trichloroethane	9.11865	0.67	1.24
1,1,2,2-Tetrachloroethane	10.84078	0.93	1.50
Hexachloroethane	14.55235	2.49	2.06
1,2-Dichloropropane	9.11069	0.57	1.24
1,2,3-Trichloropropane	10.79336	0.96	1.49
1,2,2,3-Tetrachloropropane	12.56484	1.57	1.76
Tetrachloroethylene	11.62	1.72	1.62
Trichloroethylene	9.6	1.00	1.31
4-Chlorotoluene	14.14	1.68	2.00
p,p'-DDT	30.76	4.57	4.52
1,10-Dibromodecane	25.48	2.51	3.72
1,1,2-Trichloro-1,2,2-trifluoroethane	9.85	1.70	1.35
1,2-Dibromoethane	10.48	0.35	1.45

Bromochloromethane	6.97	0.40	0.92
Bromobenzene	13.31	1.35	1.88
1,4-Dibromobenzene	16.93	2.21	2.43
1,2,4-Tribromobenzene	20.17	3.34	2.92
1,2,3,4-Tetrachlorobenzene	18.39	3.18	2.65
1,2,3,4-Tetrabromo-5-chloro-6-methylbenzene	27.26	3.98	3.99
Pentabromotoluene	28.48	3.76	4.18
4,4′-dibromobiphenyl	29.41	3.57	4.32
1,2,3,4-Tetrachloronaphthalene	26.37	3.33	3.86
Hexachlorobutadiene	19.73	3.35	2.85
1-Chlorobutane	9.51	1.15	1.30
1,1,2,2-Tetrabromoethane	16.29	1.26	2.33
1,1-Dichloroethane	7.55	0.95	1.00
Allyl chloride	7.76	0.54	1.04
4-isopropenyl-chlorobenzene	18.52	2.84	2.67
1,2,3,4,5-Pentabromo-6-chlorocyclohexane	27.58	3.1	4.04
Chlorocyclohexane	12.42	2.34	1.74
Benzotrifluoride	10.52	1.65	1.45
tetra(bromomethyl)methane	21.45	2.62	3.11
1,3-Dichlorobenzene	12.302	2.33*	1.72
1,2,4-Trichlorobenzene	14.1106	2.86*	2.00
1,2,4,5-Tetrachlorobenzene	15.9804	3.45*	2.28
3,3'-Chlorobiphenyl (PCB-11)	22.8207	2.63*	3.32
2,5-Chlorobiphenyl (PCB-9)	22.3437	3.86*	3.25
2,4,4'-Trichlorobiphenyl (PCB-28)	24.7784	4.33*	3.62
2,3,5,6-Tetrachlorobiphenyl (PCB-65)	25.55981	4.71*	3.73
2,5,2',6'-Tetrachlorobiphenyl (PCB-53)	25.13102	4.46*	3.67
2,3,3',4,4'-Pentachlorobiphenyl (PCB-105)	33.55	4.28*	4.94
2,2',4,5',6- Pentachlorobiphenyl (PCB-103)	31.25	4.58*	4.6
Trichloromethane	7.22831	0.93*	0.95
1,1,1-Trichloroethane	9.24654	0.95*	1.26
1,3,5-Tribromobenzene	20.47	3.38*	2.96
Tribromomethane	11.36	1.13*	1.61
2-Chlorotoluene	13.96	1.82*	2.00
Hexachlorobenzene	19.4794	4.26*	2.83
1,1,2,2-Tetrachloro-1,2-difluoroethane	11.9	1.78*	1.69
p,p'-DDE	35.8	4.51*	5.30
3-Chlorobenzotrifluoride	14.17	2.35*	2.03
1,2,3,4,5,6-Hexachlorocyclohexane	21.81	2.77*	3.19

Note:* training set.

Table S.4 Compounds used to correlate molecular polarizability and log BCF in microorganism

Compound	Polarizability ($Å^3$)	microorganism BCF
Chlorobenzene	10.4825	2.21
1,2-Dichlorobenzene	12.1401	2.86
1,3-Dichlorobenzene	12.302	2.86
1,2,4-Trichlorobenzene	14.1106	3.52
1,2,3,5-Tetrachlorobenzene	15.9196	3.26
Monochloromethane	3.54598	0.505
Dichloromethane	5.2984	0.778
Trichloromethane	7.22831	1.41
Tetrachloromethane	9.12655	2.32
Monochloroethane	5.5283	0.99
1,1-Dichloroethane	7.35887	1.28
1,1,1-Trichloroethane	9.24654	1.908
1,2-Dichloroethane	7.34642	0.954
1,1,2-Trichloroethane	9.11865	1.519
1,1,2,2-Tetrachloroethane	10.84078	1.96
Hexachloroethane	14.55235	3.83
Chloroethene (Vinyl chloride)	5.68	0.756
1,1-Dichloroethene	7.55	1.72
Trichloroethylene	7.74	1.68
Tetrachloroethylene	9.6	1.987
1,3-Dichloropropene	11.62	2.4
Trichlorofluoromethane	8.01	1.92
Bromomethane	4.97	0.623
Tribromomethane	11.36	1.8
Bromodichloromethane	9.04	1.544